1.1 Introduction

The word “nano” is originated from a Greek word ‘nanos’ meaning extremely small which refers to a billionth of a meter (10^{-9} meter) and deals with the size ranging from 1-100 nm. Nanotechnology is an art and science of manipulating and controlling the matter at nanoscale enabling for novel applications. It is an emerging area of science and technology which is being applied in the field of biotechnology, material science, and electronics. The concept of nanotechnology was first oozed out in the historical talk “There is a Plenty of Room at the Bottom” dated 29th Dec 1959, given by an American physicist Professor Richard Feynman where he introduced about the world in which atoms could be controlled and directed (Feynman 1960). On 5th Oct 1984, Richard Feynman repeated his lecture in a seminar entitled “Idiosyncratic Thinking” where he called his talk ‘Tiny Machines’. The term ‘Nanotechnology’ was given by Professor Norio Taniguch (Taniguchi 1974, Handy *et al*. 2008). He stated that the stock removal of a little bit size, acrretion or flow of material is of 0.1 to 0.2 nm long. Therefore, he expected the size of fineness of the order of one nm.

The materials designed or manipulated by the nanotechnology are known as nanomaterials. At present the nanomaterials are receiving huge interest of the researchers engaged in the areas of environment, energy, catalysis, biomedical, electronics, health care, cosmetics, food and feed, drug-gene delivery, mechanics, optics, chemical industries, space industries, science, light emitters, single electron transistors, nonlinear optical devices and photo-electrochemical applications.

These nanomaterials have attracted the researchers due to their extremely small size and high surface area to volume ratio. These characteristics feature differentiated the nanomaterials with the bulk materials of the same composition concerning both physical and

chemical properties like mechanical, thermal, biological, optical absorption, electrical conductivity and melting point. For instance, in nanomaterials, the optical properties such as refractive index and absorbance are directly related to the size and shape but the optical properties of the bulk material are fixed, regardless of its mass or volume. Therefore, the size and shape of the nanomaterials play a vital role in performing the novel application.

1.1.1 Types of nanomaterials

Till date, the growing field of nanotechnology has found that there is a lack of internationally agreed definition of nanomaterials and nanoparticles (Handy *et al*. 2008). However, the materials with at least one dimension having a size range between 1 nm - 100 nm are being regarded as nanomaterials.

1.1.1.1 Based on dimension

Based on dimension, Siegel has classified the nanomaterials into four categories: 0D: nanoclusters, 1D: multi layers, 2D: nanograined layers and 3D: equiaxed bulk solids (Carrow and Gaharwar 2015).

A. Zero-dimensional (0-D)

In these systems, all three dimensions lie in the nanometer range. The most common type of zero-dimensional system is nanoparticles which may be amorphous or crystalline, single crystalline or polycrystalline. The Zero-Dimensional material can be composed of single or multi-chemical elements. **Fig. 1.1** represents the different types of the zero dimensional nanostructure (Tiwari *et al*. 2012).

Example - Quantum dots, Nanoparticles, Nanospheres, etc.

B. One-dimensional (1-D)

In 1-D nanomaterials, one of the dimensions is out of the nanoscale while other two dimensions are in nanoscale which leads to the formation of needle shaped nanostructures as shown in **Figure 1.1**

Example - Nanotubes, Nanowires, and Nanorods

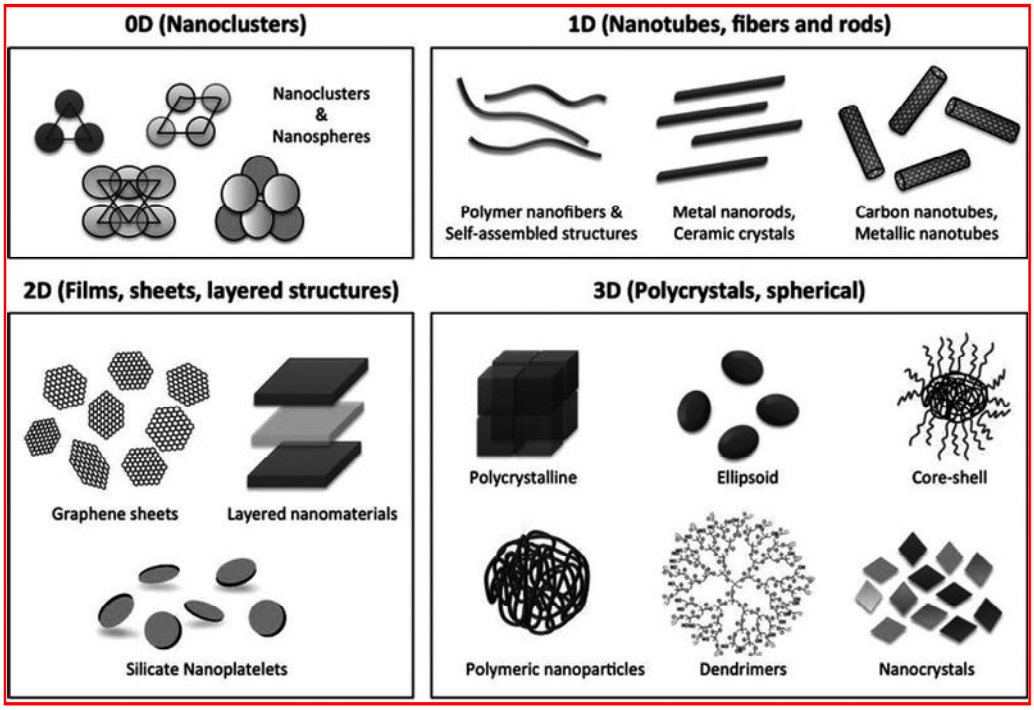

Figure 1.1 Schematic representations of structurally different dimensions of nanomaterials with suitable examples (Figure adopted from Carrow and Garhwar 2015)

C. Two-dimensional (2-D)

In 2-D nonmaterial, only one dimension is in nanoscale while other two dimensions are out of nanoscale. These nanomaterials are used as single or multilayer structures. Such nanostructures may be amorphous or crystalline in nature and made up of the various chemical compositions **(Fig. 1.1)**.

Example - Nanoplates, Graphene sheets, etc.

D. Three-dimensional (3-D)

3-D nanomaterials are not confined in nanoscale in any dimensions. These systems comprise bulk materials in which all the dimensions are in macroscale. A bulk material concerning the nanocrystalline structure is made up of several nanosized crystals. 3-D nanomaterials are composed of a multiple arrangement of nanosize crystals, most typically in different orientations. 3-D nanomaterials may contain dispersions of nanoparticles, bundles of nanowires, and nanotubes as well as multinanolayers **(Fig 1.1).**

Example - Bulk material, Nanoflowers, Nanocone, etc.

1.1.1.2 Based on core source material

On the basis of the core source material, the nanomaterials can be broadly categorized into (A) Carbon-based nanomaterials, (B), Metal oxide nanomaterials, (C) Metallic nanomaterials.

A. Carbon-based nanomaterials

The carbon-based nanomaterials like, Fullerene, Carbon Nanotubes (CNTs), Graphene, have revealed greater potential in various applications such as biosensing, electronics, optics, and biomedicine.

Fullerene was first discovered by Krato *et al*., in 1985 by vaporizing the graphite using Nd:YAG laser (Kroto *et al*. 1985). Since the discovery of the fullerenes, it has drawn much attention of the scientists due to potential application in several fields such as biomedicine (Gharbi *et al*. 2005), drug delivery (Yang *et al*. 2017), and solar cells (Thompson and Fréchet 2008).

CNTs can be visualized as a sheet of graphite, which has been rolled up into a cylindrical tube (Tasis *et al*. 2006). The length of CNTs is in the size of micrometers with diameters up to 100 nm (Thostenson *et al*. 2001). Because of having some exceptional physicochemical properties such as mechanical, electrical, thermal, and optical properties, the CNTs are being widely used in catalyst, semiconductor, automotive and energy harvesting industries (Pokhrel *et al*. 2017).

Graphene is considered as an essential building block of all graphitic forms such as CNTs, fullerenes, and graphite (Wang *et al*. 2012). It is a sp^2 hybridized two-dimensional sheet of single-atom thick carbon which possesses extraordinary chemical, electrical, mechanical properties, rapid electron transfer kinetics and significant electrocatalytic characteristics (Novoselov *et al*. 2012). Due to these unique properties, it is being used in different applications like bioimaging, biosensing, energy storage, electronic devices, environmental treatment, therapeutic drug/gene delivery, stem cell, and tissue engineering, etc. (Cheng *et al*. 2017).

B. Metal oxide nanoparticles

Recently, the metal oxide nanoparticles (MONPs) have attracted the researchers because of some unique properties such as increased surface area to volume ratio, high surface energy, energy, and strong surface absorption (Santos *et al*. 2016). Due to these properties, the MONPs are widely used in various fields such as chemistry, materials and engineering, as well as in the frontiers of medicine (Koch *et al*. 2007). These MONPs are iron oxide nanoparticles (IONPs), cerium oxide nanoparticles (CeONPs), titanium dioxide nanoparticles (TiONPs), zinc oxide nanoparticles (ZnONPs), etc. These can be synthesized through several methods such as chemical vapor deposition, laser ablation, photolithography,

thermal decomposition, sol-gel process or hydrothermal reaction method and biological methods. IONPs have revealed its potential towards the biomedical applications such tissue repair, drug delivery, magnetic resonance imaging (MRI) and hyperthermia (Gupta and Gupta 2005, Laurent *et al*. 2008, Qiao *et al*. 2009, Cano *et al*. 2017). CeO_2 nanoparticles have shown mimetic properties of catalase oxidase, peroxidase, superoxide oxidase, and have emerged as a fascinating material in biological fields, such as in drug delivery bioanalysis, and biomedicine (Charbgoo *et al*. 2017, Naganuma 2017). TiO_2 is used in printing ink, water purification, UV sunscreens, cosmetics, medical implants, and sensors (Pakrashi *et al*. 2014, Chen and Mao 2007). In addition to these, TiO_2 is also used in several applications such as catalysis, photovoltaics, fuel cells, optoelectronics, batteries, smart windows, self-cleaning and antifogging surfaces. ZnONPs is widely used in various fields such as electronics, optoelectronics, photo-catalysis and laser technology (Lu *et al*. 2015, Yang and Park 2007). In addition to this, ZnONPs is also used in ceramics industry because of its hardness, rigidity and piezoelectric constant.

C. Metallic nanoparticles

Metal nanoparticles (MNPs) have been a favorite topic of the researchers engaged in nanoscience and technology at global scale due to their diverse applications in various fields of science and engineering. Among various MNPs, gold (Au), silver (Ag), palladium (Pd), and platinum (Pt) nanoparticles (NPs) are widely used in various applications. A brief description on these is given below.

Platinum is a precious noble metal and its salt, i.e. cis-diammine dichloro platinum is used as a cancer drug (Tahir *et al*. 2017). The PtNPs are used in fuel cells and hydrogen storage materials. PtNPs acts as a significant catalyst than bulk materials (Schmidt *et al*.

1999, Cheng *et al*. 2009). Several platinum-based complexes are being used against both gram-positive and gram-negative bacteria as a potent antibacterial agent (Sharma 2017).

Pd is a member of platinum group metals (PGMs) which is least dense and has lowest melting point out of all the PGMs. The PdNPs show excellent catalytic activity and have been used extensively as a catalyst in the field of catalysis (Li *et al*. 2017). In addition to this, PdNPs are also used in different applications such as carbon-carbon coupling reaction, oxidation, hydrogenation, electrochemical reactions in fuel cells, hydrogen storage, and gas sensing (Ismail *et al*. 2017).

AgNPs are one of noble metal nanoparticles of (NMNPs) and are of great interest and have attracted intensively because of their enormous applicability in antibacterial, antiviral and anticancer therapies (Saxena *et al*. 2012, Lu *et al*. 2008, Rahban *et al*. 2010). In addition, AgNPs are also used in biosensing, catalysis, water treatment, wound dressings, medicine and surgical instruments (Dahl *et al*. 2007, Dubas and Pimpan 2008, Filippo *et al*. 2010, Vivek *et al*. 2012). Recently, Francis *et al*. has prepared the AuNPs using *Mussaenda glabrata* leaf extract and examined in catalytic degradation of dye rhodamine B and methyl orange and reduction of 4-nitrophenol (Francis *et al*. 2017).

Since last decades, the gold nanoparticles (AuNPs) have played an important role in the various areas such as biosensing, catalysis, anticancer, medicine, electronics etc. (Varun *et al*. 2017, Shen *et al*. 2017, Ramachandran *et al*. 2017, Ribeiro *et al*. 2017, Daniel and Astruc 2004). It can be also synthesized through several routes like physical, chemical and biological where the physical and chemical routes suffered by the several environmental pollution issues, costly instrumentation and energy consumption while heating and stirring.

The principles of green chemistry have played a major role in biological (green) synthesis of AuNPs by involving green route using algae (González-Ballesteros *et al.* 2017), fungi (Pei *et al*. 2017), bacteria (Ojo *et al.* 2016), and plants (Pourmortazavi *et al*. 2017).

1.2 Synthesis of nanoparticles

The different method of preparation of nanoparticles is usually classified into two broad categories: (1) top-down and (2) bottom-up which is based on the processes involved in the creation of the nanoscale structures (**Scheme 1.1**).

1.2.1 Top-down Method

The top-down method involves the reduction of the size of suitable starting bulk material up to nano-range using physical or chemical means (**Scheme. 1.2**). The imperfection of the surface structure is the major drawback of this method which significantly affects the physical properties as well as the surface chemistry of the nanoparticles due to the high aspect ratio (Thakkar *et al*. 2010). It is governed by several methods like mechanical milling, laser ablation, arc discharge, and chemical methods such as templated etching, selective dealloying, anisotropic dissolution, and thermal decomposition.

1.2.2 Bottom-up method

Bottom-up, approach refers to the construction of a structure atom-by-atom, molecule-by-molecule, or cluster-by-cluster (Thakkar *et al*. 2010). In this approach, initially, the nanostructured building blocks (i.e. nanoparticles) are formed and, subsequently, assembled into the final material using chemical or biological procedures for synthesis **(Scheme. 1.2)**. A distinct advantage of the bottom-up approach is the enhanced possibility of

obtaining metallic nanoparticles with comparatively lesser defects and more homogeneous chemical compositions.

Nucleation and growth are two interesting phenomena of a bottom-up approach. The bottom-up approach is followed by several steps. The first step is the reduction of metal ions (M^+) to zero valent metal ion (M^0) via the electrons produced by the reductant.

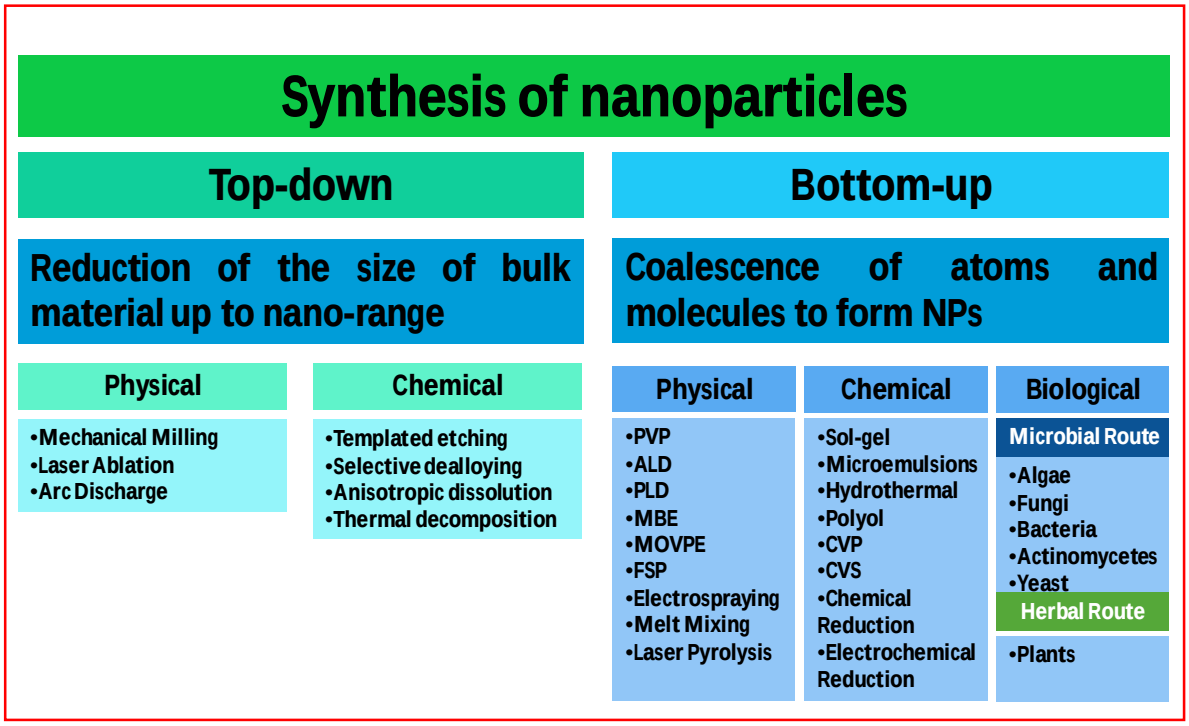

Scheme 1.1 Graphical representation of different top-down and bottom-up synthesis approaches

The concentration of the M^0 continued to increase with the continued reduction of M^+. When the increased concentration of M^0 atoms exceeded the critical supersaturation, the M^0 started to nucleate and formed the crystal nuclei (step II). The formation of these crystal nuclei led to the decrease in concentration of M^0 atoms below to the critical supersaturation where the whole process is dominated by the growth of nuclei to form nanoclusters because

of no longer increase in a number of crystal nuclei (step III). The growth of the nanoclusters further decreased the concentration of M^0 atoms below the saturation level which stopped the growth of nanoclusters and finally aggregated to form MNPs (step IV) which is shown in Scheme 1.3 (Tran and Nguyen 2011).

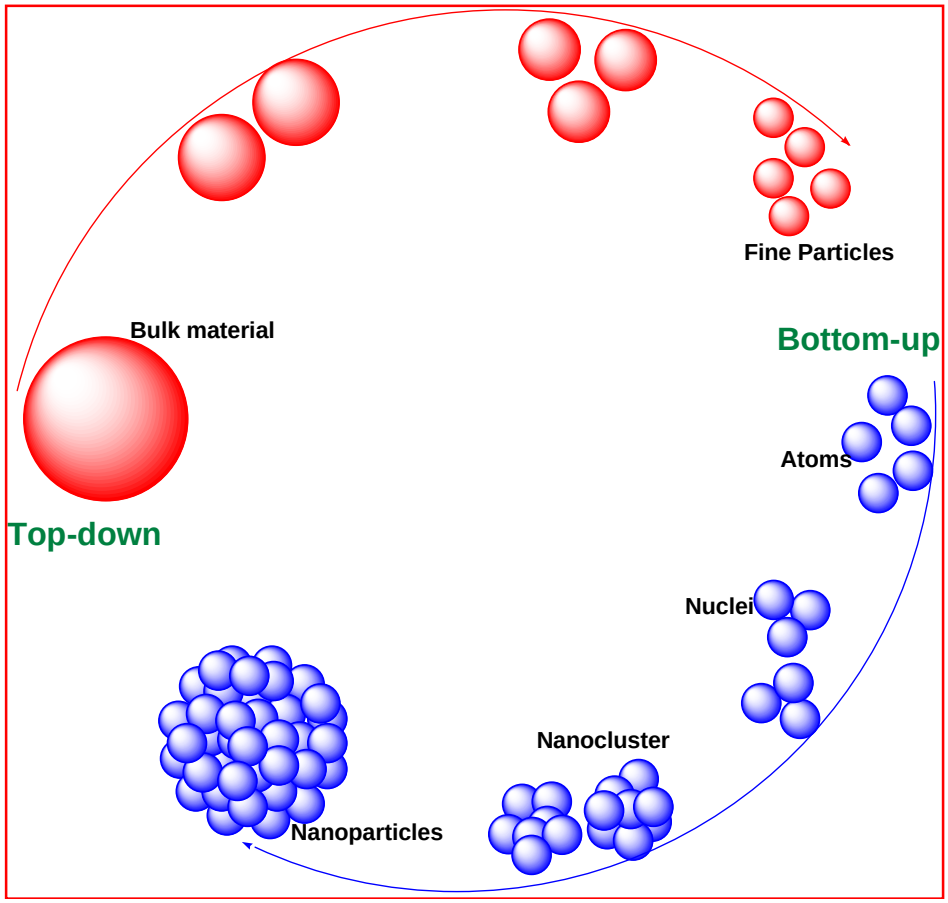

Scheme 1.2 Schematic representation showing (a) top-down and (b) bottom-up approach of nanoparticles synthesis

Botton-up techniques can be perforemed by several methods such as sol-gel, microemulsions, hydrothermal, solvothermal, physical vapor deposition (PVD), chemical vapor deposition (CVD), chemical vapor synthesis (CVS), photochemical, sonochemical, chemical and electrochemical reduction, biological.

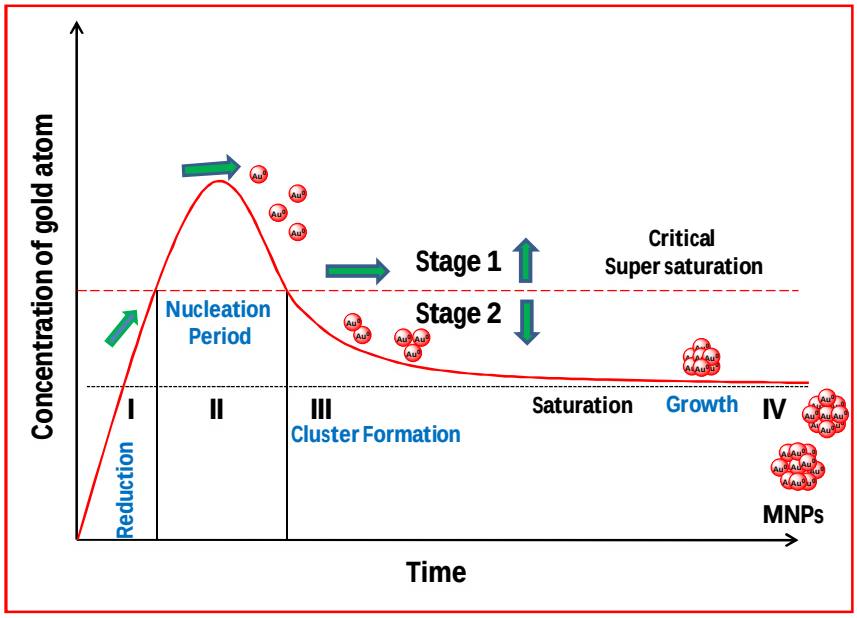

Scheme 1.3 La Mer mechanism of the nucleation of atoms, their pattern of changing concentration with time and further growth to form nanoparticles

1.3 Overview of AgNPs and AuNPs

1.3.1 AgNPs

Silver is one of the eight noble metals or precious metals which are called as PGMs. It is soft, malleable, and most ductile metals which made it use into fashioned items such as different kind of jewelry and various decorative items. Ag belongs to 4d transition element having atomic number 47, atomic weight 107.87, and electron configuration [Kr] $4d^{10}5s^{1}$ which is located in period 5 and group 11 in the periodic table. Silver exists in four oxidation states which are 0, +1, +2, and +3. The +1 is the common state of silver, 0 and +2 are uncommon whereas +3 persists only in the formation of the complex. Natural silver is a comprised of two stable isotopes Ag^{107} and Ag^{109} which shares 51.82% and 48.18% respectively. The face-centered cubic crystal structure is very common crystal structure of silver which has a melting point 961.8 °C and boiling point 2162 °C.

Silver is an inert element which does not react with atmospheric oxygen easily, but it is the most permeable of metals to atomic oxygen; molten silver dissolves almost ten times its volume of oxygen. However, it readily forms tarnish surface by reacting with sulfurous gases. Silver dissolves in the presence of oxygen in solutions of potassium or sodium cyanide and in oxidizing acids. Mostly, the compounds of silver are based on Ag (I), and most of them are insoluble and soluble in aqueous environments. Only a few compounds of Ag (II) are known, whereas no any simple compounds of Ag (III) exist. Ag (I) and (II) also form complexes with ammonia, cyanide, halide ions, thiosulfate and thiourea and with many organic aromatics and olefins. Silver nitrate ($AgNO_3$), Silver bromide (AgBr), and Silver chloride (AgCl) are some silver compounds of principal commercial interest.

$AgNO_3$ is the most important commercial compound of Ag (I) and is the intermediate chemical from which all other silver compounds are made. It is prepared by the dissolution of silver metal in hot nitric acid. The purified crystalline nitrate is not photosensitive, but it is easily reduced to metal by formaldehyde, glucose, and several other reagents. AgBr is yellow to a green-yellow crystalline compound which is more photosensitive than the AgCl or AgI and hence, it is widely used for photographic emulsions. AgCl is a white crystalline photosensitive material that is widely used in photographic papers. AgI is less photosensitive than AgBr or AgCl but is responsive to a wider span of the visible spectrum. It is also used extensively in photographic materials and sea water-activated batteries. Silver oxide (Ag_2O) is used in standard silver batteries. The Ag (II) tetroxide (Ag_4O_4) is an oxidizer used to kill bacteria in cooling system water and swimming pools (Etris 1997).

Silver is a positively charged cation (Ag^+) having ionic radius of ~0.1 nm which are not considered as a particle. Due to presence of a single charge (Ag^+) they are highly reactive. They can associate with other ions but cannot be destroyed because these ions are inherently persistent. The silver ions and AgNPs are fundamentally different because AgNPs can dissolve or disaggregate and can lose the properties of particles. The term colloid is also applied to AgNPs. Colloid indicated to the particles in a wide range between 1 nm and 1,000 nm ie. a colloid may or may not be a nanoparticles. AgNPs refer to a particle which contains several silver atoms. AgNPs are usually engineered to release silver ions, which are the source of potential antibacterial activity.

1.3.2 AuNPs

Gold is also one of the eight noble metals or precious metals generally called as PGMs. Gold is the most ductile and malleable element on our planet. It bears the characteristic property of sectility which could be stretched into a wire, cut into slices, and pounded into other shapes. It is an excellent metal for jewellery because it never tarnishes. Gold belongs to 5d transition element having atomic number 79, atomic weight 196.6, and electron configuration [Kr] $5d^{10}6s^1$ which is located in period 6 and group 11 in the periodic table. Gold exist in six oxidation states which are 0, -1, +1, +2, +3, and +5 (Puddephatt and Vittal 1994). The free +1 is unstable in solution form and prefers to form two ($K^+AuCl_2^-$, $K^+Au(CN)_2$) or four $(K^+[A(dipy)(CN)_2])^-$ coordinate systems. The +3 is most common state of gold which is present in four coordinate square planner complexes such as $K^+AuCl_4^-$. It is also present in five and six coordinate Au (III) complexes such as $[Au(diars)_2I]^{2+}(C1O_4)^{2-}$ and $[Au(diars)_2I_2]^{2+}(C1O_4)^-$ respectively. The compounds, Rb_5Au_3O and M_7Au_5O reflect -1 oxidation state of gold. The +2 oxidation state of gold is very and present in

$[(C_2H_5)_4N]Au(II)(B_9C_2H_{11})_2$ whereas +5 state is present in Cs^+AuF6^- and $O_2^+AuF_6^-$. Gold shows 0 oxidation state in its pure elemental form ($[Au_9(PPh_3)8](NO_3)_3$. The melting and boiling point of gold is 1,064 °C and 2,700 °C respectively which has face-centered cubic (fcc) crystal structure (Pyykkö 2004, Puddephatt 1978). The chloroauric acid ($HAuCl_4.\mathbf{x}H_2O$) is commercially available salt of gold which used widely for the preparation of AuNPs. Gold is a positively charged cation (Au^{3+}) which is not considered as a particle. The gold ions and AuNPs are totally different because AuNPs can dissolve or disaggregate and can lose the properties of particles. AuNPs refer to a particle which contains several silver atoms of elemental gold which is obtained by the reduction of Au^{3+} to Au^0.

1.3.3 History of AgNPs and AuNPs

The preparation and utilization of the AgNPs and AuNPs have a very long history since millennia. The AgNPs and AuNPs have been used by our ancient civilization because their extraordinary properties like optical and curing properties were known to them. The preparation of the gold solution was first mentioned by Egyptians and Chines by 5th century BC. The solutions of the silver and gold have been used by Romans to color the glass of intense shades of red, yellow and mauve using their different concentrations. The Romans used to add gold salt during the preparation of the glass which when annealed, get reduced to colloidal gold solution having intense ruby color. The intense ruby color of the gold solution appear due to the nucleation and further growth of AuNPs having a optimum size range 5-60 nm (Wagner *et al*. 2000). The excellent example of the utilization of AgNPs and AuNPs is the Lycurgus cup of 4th century which is presently in British Musium **(Fig. 1.2)**. This Lycurgus cup have extraordinary optical effect displayed by the glass which appears as deep wine red in transmittance light whereas opaque pea-green in reflected light.

Figure 1.2 Lycurgus cup (British Museum; AD 4th century). The colloidal gold causes the glass to appear opaque pea green in reflected light and wine red (ruby red) in transmitted light

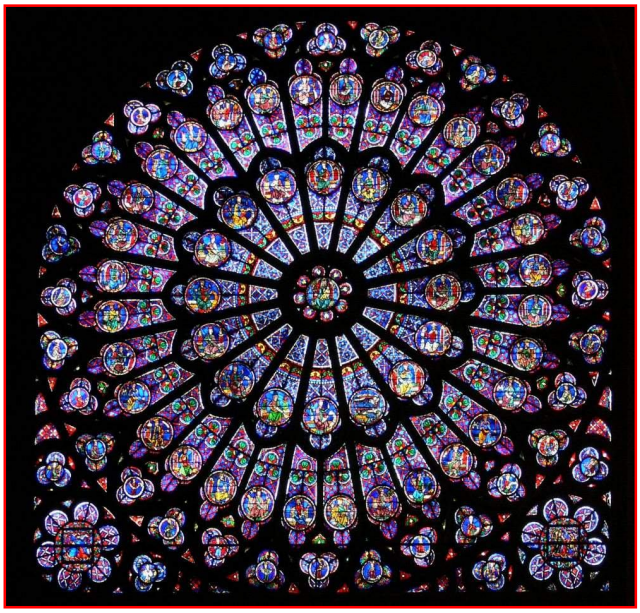

Figure 1.3 Gothic stained glass rose window of Notre Dame de Paris. The red colors were due to the colloids of AuNPs

The chemical analyses of the dichoric color of the glass attributed to the surface plasmon resonance (SPR) of the nanocrystals of gold and silver alloy dispersed throughout the matrix of the glass. The stained window glass in Europian cathedrals is similar example using colloidal metal nanoparticles. In the middle Ages, the artisian started to use colloidal gold for the production of stained glass window having red and purple color. For example the rose window of the Cathedral of Notre Dame with red and purple hues is due to the presence of gold colloid **(Fig. 1.3)**. The porcelain prepared in 15^{th} century was also an example of using colloid of silver and copper. The technique of preparing porcelain was developed in Islamic world during 9^{th} century where the nanoparticles were formed by the reduction of the metal salts previously deposited on the ceramic piece from a vinegar solution. The coloring of the glass process was further refined by the contriving of "Purple of Cassius" which is a precipitate of colloidal gold and stannic hydroxide (Ferrari 2005). Michael Faraday has reported the first scientific study of the synthesis of MNPs in 1850 by the reduction of the $AuCl_4$ by phosphorus in the presence of carbon disulphide with the already reported method by Paracelsus in 16^{th} century for "Aurum Potabile". Faraday was the first who found out that the minute size of the gold particles was responsible for the red color of the solution. In 1906, Zsigmondy has prepared the monodispersed gold sol by the reduction of chloroauric acid using formaldehyde (Zsigmondy 1906). In 1917, he also investigated the rapid synthesis of monodispersed AuNPs using Faraday gold sol as a seed crystal (Zsigmondy 1906).

In 1951, Turkevitch improved the method of Zsigmondy through the synthesis of hydrophilic AuNPs by the reduction of chloroauric acid using sodium citrate in a boiling aqueous solution. The citrates adsorbed on the surface of the AuNPs and thus act as a capping agent. The TEM used for the analysis of the AuNPs thus produced revealed that the

average diameter of the particles was from 20±1.5 nm (Turkevich *et al*. 1951). This work was further refined by Frens who examined the effect of concentration of citrate on the size of the AuNPs and obtained the particles in the range of 16-147 nm. After that, the Turkevitch method was also used for the synthesis of silver nanoparticles. In early 1990, Brust *et al*. have represented a two-phase liquid-liquid system to prepare colloidal gold in an organic solvent which was not miscible in water (Brust *et al*. 1994). In recent years several modified and additional procedures have been developed for the synthesis of AgNPs and AuNPs with controlled shape and size.

1.4 Green synthesis of AgNPs and AuNPs

Since last decades, the development of green synthesis has become an essential branch of nanotechnology and has received a considerable attention of the researchers engaged in the synthesis of MNPs especially; AgNPs and AuNPs. Green synthesis is an environment-friendly and cost-effective method which can be scaled-up for large scale synthesis. It avoids the need of high temperature, pressure, energy, sophisticated instrumentations, technical expertize as well as the hazardous reducing agent such as hydrazine hydrate ($N_2H_4.H_2O$), sodium borohydrate ($NaBH_4$), N, N-dimethyl formamide (DMF) and sodium citrate ($Na_3C_6H_5O$). The green synthesis involves the principles of the green chemistry which aim at its utilization through reducing or eliminating the use or production of chemical hazardous to the environment. The main aim of the green chemistry regarding the synthesis of AgNPs and AuNPs is to follow the safest, fastest and cheaper route for their efficient synthesis. The green synthesis of silver and gold is performed through microbial route using bacteria, fungi, algae, yeast and phyto-mediated route using different parts of the plants.

1.4.1 Microbial route

The microbes like bacteria, fungi, algae, and yeast can synthesize AgNPs and AuNPs either intracellularly or extracellularly. The intracellular synthesis occurs inside the cells, in cytoplasm or cytosol. In intracellular synthesis, the metal ions are accumulated inside the cells by the organisms which are then reduced to particular metallic nanoparticles in the presence of optimum parametric conditions. This process of synthesis MNPs is known as biomineralization (**Scheme 1.4**). The major limitation of the intracellular synthesis of nanoparticles is a requirement of additional steps such as ultrasound treatment or reactions with suitable detergents to release the synthesized nanoparticles (Kalimuthu *et al*. 2008).

The enzyme nitrate reductase plays a very critical role in nitrogen cycle which converts nitrate to nitrite which is an NADPH-dependent enzyme and has been found to be responsible for the intracellular synthesis of MNPs (Durán *et al*. 2005). During the catalysis reaction, the nitrate reductase converts nitrate into nitrite, with the ejection of an electron which reduces the M^+ to M^0. The intracellular synthesis of AuNPs by *Verticillium sp* reported by Mukherjee *et al*. occurred due to enzyme activity occurring at the cell membrane (Mukherjee *et al*. 2001). The intracellular synthesis of AgNPs has been shown in the organism *Bacillus licheniformis* which is known to secrete the cofactor NADH and nitrate reductase; NADH-dependent enzymes, which is involved in the reduction of Ag^+ to Ag^0 and subsequently formed AgNPs after further growth (Kalimuthu *et al*. 2008). The involvement of nitrate reductase in the synthesis of AgNPs is shown in **Scheme 1.4**. The direct role played by nitrate reductase for the synthesis of AgNPs was first reported by Kumar *et al.* who used the purified nitrate reductase obtained from *Fusarium oxysporum* for the synthesis of AgNPs

(Kumar *et al*. 2007). The reaction mixture used by Kumar *et al*. contained only the enzyme nitrate reductase, silver nitrate solution, and NADPH which turned brown.

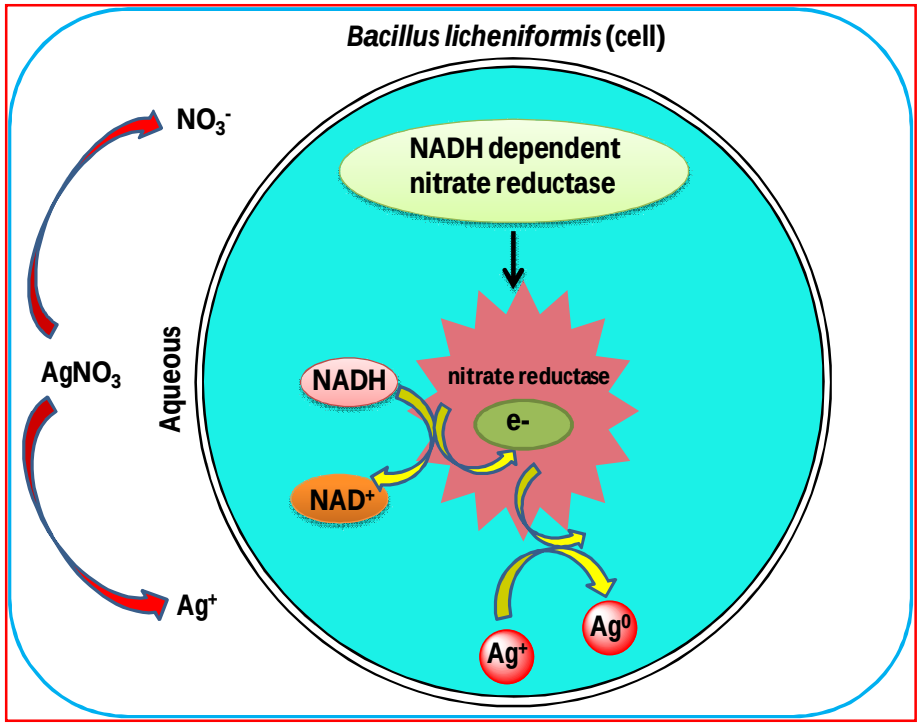

Scheme 1.4 Mechanism of intracellular synthesis of AgNPs by *B. licheniformis* showing the reduction of Ag^+ to Ag^0 via the electron shuttle enzymatic reduction process through NADH-dependent reductase as a carrier of electrons from NADH

The extracellular synthesis occurs outside the cells. It is cheap, and it requires simpler downstream processing than intracellular synthesis and favors large-scale production to explore the potential applications of MNPs. In extracellular biosynthesis, two different preparation methods are used: rapid synthesis and slow synthesis. The former occurs in few minutes whereas the latter occurs in several hours or even days. For example; the synthesis of AgNPs using culture supernatant of *Klebsiella pneumoniae* occurred in 5 minutes which is a

rapid synthesis (Mokhtari *et al*. 2009). The synthesis of AgNPs driven by the mycelial mat of *Phaenerochaete chrysosporiom* in 24 hours is regarded as a slow synthesis.

1.4.1.1 Bacteria

Among several microorganisms, bacteria are considered as the potential biofactory for the green synthesis of AgNPs and AuNPs. Some microorganisms are resistant to high metal ion concentration therefore they can survive at high concentration due to mechanisms like efflux systems, alteration of solubility, toxicity via reduction or oxidation, biosorption, bioaccumulation, extracellular complexation or precipitation of metals and lack of specific metal transport systems. Hence survive at higher concentration and able to reduce the metal ion into their metallic form. Klaus *et al*. and Joerger *et al*. have reported the synthesis of AgNPs (3-200 nm) using bacterium *Pseudomonas stutzeri* AG 259 isolated from silver mines (Klaus *et al*. 1999, Joerger *et al*. 2000). Nair and Pradeep have synthesized nanoparticles of silver, gold and their alloys using the *Lactobacillus sp* (Nair and Pradeep 2002). Zhang *et al*. also reported the adsorption and reduction of diamine silver complex using the *Corynebacterium* strain SH09 (Zhang *et al*. 2005). Shahverdi *et al*. reported the rapid formation of AgNPs using the culture supernatants of different *Enterobacteria strains* (Shahverdi *et al*. 2007). This strain showed strong biosorption towards $[Ag(NH_3)_2]^+$ at 60 ºC and reduction of Ag^+ to Ag^0 to form the nanoparticles of size 10-15 nm. Their study showed that the ionized carboxyl of amino acid residues and the amide of the peptide chains were responsible for adsorption of $[Ag(NH_3)_2]^+$ onto the cell wall of *Corynebacterium* strain's SH09. Whereas the reduction of $[Ag(NH_3)_2]^+$ to Ag^0 was due to the aldehyde or ketone which

Table 1.1 List of bacterial strains used in the biosynthesis of AgNPs

Bacteria	Precursor	Intracellular/ Extracellular	Size (nm)	Morphology	Application	Reference
Pseudomonas stutzeri AG259	$AgNO_3$	Intracellular	200	Anisotropic	-	Klaus *et al*. 1999
Pseudomonas stutzeri AG259	$AgNO_3$	Intracellular	5-100	Anisotropic	-	Joerger *et al.* 2000
Lactobacillus Strains	$AgNO_3$, $HAuCl_3$	Intracellular/ Extracellular	20-50	Anisotropic	-	Nair and Pradeep 2002
Corynebacterium strain SH09	$AgNO_3$	Intracellular	10-15	Spherical	-	Zhang *et al*. 2005
Klebsiella pneumonia, *Escherichia coli*, and *Enterobacter cloacae*		Extracellular	52.5	Spherical	-	Shahverdi *et al*. 2007
Morganella sp	$AgNO_3$	Extracellular	20±5	Spherical	-	Parikh *et al.* 2008
Bacillus licheniformis	$AgNO_3$	Intracellular	50	Spherical	-	Kalimuthu *et al*. 2008
Klebsiella pneumoniae	AgCl	Extracellular	3	Spherical	-	Mokhtari *et al*. 2009
Proteus mirabilis PTCC 1710	$AgNO_3$	Intracellular/ Extracelluar	10-20	Spherical	-	Samadi *et al*. 2009
Bacillus licheniformis	$AgNO_3$	Intracellular	50	Spherical	-	Gurunathan *et al.* 2009
Shewanella oneidensis	$AgNO_3$	Extracellular	4±1.5	Spherical	-	Suresh *et al.* 2010
Lactobacillus casei	$AgNO_3$	Extracellular	25–50	Spherical	-	Korbekandi *et al.* 2012
Klebsiella pneumoniae	$AgNO_3$	Extracellular	15-37	Spherical	-	Kalpana and Lee 2013
Escherichia coli DH5α	$AgNO_3$	Extracellular	10-100	Spherical	-	Ghorbani, 2013
Serratia nematodiphila	$AgNO_3$	Extracellular	10–31	Spherical	-	Malarkodi *et al.* 2013
Bacillus strain CS 11	$AgNO_3$	Extracellular	42-92	Spherical	-	Vindhya Lakshmi *et al.* 2014
Penicillium glabrum (MTCC 1985)	$AgNO_3$	Extracellular	26–32	Spherical	-	Nanda and Majeed 2014
Endosymbiotic bacterium	$AgNO_3$	Extracellular	10–60	Spherical	-	Yashwantha Rao *et al.* 2016
Pseudomonas aeruginosa DM1	$AgNO_3$	Extracellular	45-100	Anisotropic	-	Kumari *et al.* 2017

further grew into AgNPs after the nucleation and cluster formation. Parikh *et al*. reported the synthesis of AgNPs using a bacterium isolated from an insect gut *Morganella sp.* (Parikh *et al*. 2008). The biosynthesis of AgNPs was investigated by Kalimuthu *et al*. using the bacterium *Bacillus licheniformis*. They performed in-situ synthesis of AgNPs by adding the biomass of *Bacillus licheniformis* into the 100 mL solution of $AgNO_3$ at 37 ºC for 24 hrs which showed dark brown color. They obtained the synthesized AgNPs by ultrasonic disruption of the cells (Kalimuthu *et al*. 2008). The authors have demonstrated that piperitone had partially inhibited the reduction of Ag^+ by supernatants of *Klebsiella pneumoniae* and other different strains of *Enterobacteriaceae*. Mokhtari *et al*. have used *Klebsiella pneumoniae* and synthesized spherical AgNPs having average size 3 nm (Mokhtari *et al*. 2009). Samadi *et al*. studied the synthesis of AgNPs using bacteria *Proteus mirabilis* PTCC 1710 and found significant results (Samadi *et al*. 2009). It is well established fact that the electronic and optical properties of metal MNPs depend on their size and shape. Gurunathan *et al*. reported the effect of $AgNO_3$ concentration, reaction temperature and pH on the size of AgNPs (Gurunathan *et al*. 2009). Kalpana and Lee have synthesized AgNPs using cultural filtrate of simulated microgravity grown *Klebsiella pneumonia* for bactericidal acitivity (Kalpana and Lee 2013). Kumari *et al*. have shown the utilization of secondary metabolite pyoverdine from *Pseudomonas aeruginosa* DM1 for the eco-friendly synthesis of AgNPs (Kumari *et al*. 2017). Similarly, several other bacteria used for the synthesis of AgNPs are shown in **Table 1.1** (Suresh *et al*. 2010, Malarkodi *et al*. 2013, Yashavantha Rao *et al*. 2016, Ghorbani 2013)

The potential applications of AuNPs in several fields have attracted the researchers to much extent for its synthesis. Over thirty-seven years ago, Beveridge and Murray reported

the synthesis of AuNPs in the range of 5-25 nm using *Bacillus subtilis* 168 (Beveridge and Murray,1980). Since then, a number of bacteria have been used for the preparation of AuNPs from aqueous chloroauric acid solution ($HAuCl_4$) either intra or extracellularly. For example, the extracellular biosynthesis of AuNPs was reported by Ahmad *et al*. from the novel extremophilic actinomycete, *Thermomnospora sp* (Ahmad *et al*. 2003a). Gericke and Pinches have investigated the intra and extracellular green synthesis of AuNPs using *Verticillium luteoalbum*. They observed that the synthesized AuNPs were anisotropic with average size 100 nm (Gericke and Pinches 2006a). Husseiny *et al*. reported the extracellular synthesis of AuNPs using various strains of *Pseudomonas aeruginosa* (Husseiny *et al*. 2007). Deplanche and Macaskie have also reported the microbial precipitation of gold using *E. coli* and *Desulfovibrio desulfuricans* (Deplanche and Macaskie 2008). Wen *et al*. and He *et al*. have showed the extracellular synthesis of AuNPs using *Bacillus megatherium D01* and *Rhodopseudomonas capsulate* respectively (Wen *et al*. 2009, He *et al*. 2008). The intracellular synthesis of spherical AuNPs was also performed by Du *et al*. using *Escherichia coli* DH5α and obtaine the spherical AuNPs with average size 25±8 nm (Du *et al*. 2007). The preparation of anisotropic AuNPs was performed by Nangia *et al*. 2009 using *Stenotrophomonas maltophilia* (Nangia *et al*. 2009). Suresh *et al*. have reported the green and economical synthesis of AuNPs in the range of 15±5 nm using culture supernatant of *Shewanella oneidensis* (Suresh *et al*. 2011). The cell-free extract of thermophilic bacterium *Geobacillus stearothermophilus* revealed excellent potential towards the reduction of both Ag^{+} and Au^{3+} ion into Ag^{0} and Au^{0} respectively to form AgNPs and AuNPs (Fayaz *et al*. 2011a). Malhotra *et al*. have isolated novel marine bacteria *Stenotrophomonas* for the synthesis of both AgNPs and AuNPs (Malhotra *et al*. 2013). Wadhwani *et al*. have

synthesized AuNPs using *Gordonia amicalis* HS-11 sps in size range of 19-39 nm (Wadhwani *et al*. 2014).

Table 1.2 List of bacterial strains used in the biosynthesis of AuNPs

Bacteria	Precursor	Intracellular/ Extracellular	Size (nm)	Morphology	Application	Reference
Bacillus subtilis 168	$HAuCl_4$	Intracellular	-	Anisotropic	-	Beveridge and Murray,1980
Thermomonospora sp.	$HAuCl_4$	Extracellular	8-40	Spherical	-	Ahmad *et al.* 2003
Verticillium luteoalbum	$HAuCl_4$	Intracellular /Extracellular	100	Anisotropic	-	Gericke and Pinches, 2006
Pseudomonas aeruginosa	$HAuCl_4$	Intracellular	15-40	Spherical		Husseiny *et al*. 2007
Escherichia coli and *Desulfovibrio desulfuricans*	$HAuCl_4$	Intracellular	20-50	Spherical	-	Deplanche and Macaskie, 2008
Bacillus megatherium D01	$HAuCl_4$	Extracellular	2.5	Spherical	-	Wen *et al.* 2008
Rhodopseudomonas capsulata	$HAuCl_4$	Extracellular	10-20	Spherical	-	He *et al*. 2008
Escherichia coli DH5α	$HAuCl_4$	Intracellular	25±8	Spherical	-	Du *et al*. 2008
Stenotrophomonas maltophilia	$HAuCl_4$	Extracellular	40	Anisotropic	-	Nangia *et al.* 2009
Shewanella oneidensis	$HAuCl_4$	Extracellular	15±5	Spherical	-	Suresh *et al.* 2011
Pseudomonas denitrificans	$HAuCl_4$	Extracellular	25-30	Spherical	-	Mewada *et al.* 2012
Stenotrophomonas	$HAuCl_4$, $AgNO_3$	Extracellular	10-50, 40-60	Spherical	-	Malhotra *et al.* 2013
Acinetobacter sp. SW30	$HAuCl_4$		20±10	Anisotropic	-	Wadhwani *et al.* 2014
Streptomyces sp.	$HAuCl_4$	Extracellular	8.4, 10	Anisotropic	-	Składanowski *et al.* 2017

Recently, Składanowski *et al*. have reported the synthesis of AuNPs using the biomass and supernatant of *Streptomyces sp.* isolated from acid forest soil (Składanowski *et al*. 2017) which is given in **Table 1.2**

1.4.1.2 Fungi

The bioaccumulation capacity, tolerance, high binding capacity, and intracellular uptake have made the Fungi as a potent agent for the synthesis of MNPs (Sastry *et al*. 2003).

Table 1.3 List of fungal stains used in the biosynthesis of AgNPs

Fungi	Precursor	Intracellular /Extracellular	Size (nm)	Morphology	Application	Reference
Verticillium	$AgNO_3$	Intracellular	25±12	Spherical	Antifungal	Mukhergee *et al*. 2001
Phoma sp3.2883	$AgNO_3$	Intracellular	71.06± 3.46	Spherical	-	Chen *et al*. 2003
Aspergillus fumigatus	$AgNO_3$	Extracellular	5-25	Irregular	-	Bhainsa and D'Souza, 2006
Fusarium oxysporum	$AgNO_3$	Extracellular	-	Spherical	Antibacterial	Duran *et al*. 2007
Fusarium semitectum	$AgNO_3$	Extracelluar	10-60	Spherical	Medical	Basavaraja *et al*. 2008
Fusarium acuminatum	$AgNO_3$	Extracellular	13	Spherical	-	Avanish *et al*. 2008
Penicillium brevicompactum W A 2315	$AgNO_3$	Extracellular	23-105	Irregular	-	Avanish *et al*. 2008
Penicillium fellutanum	$AgNO_3$	Extracellular	-	Spherical	-	Kathiresan *et al*. 2009
Alternaria alternata	$AgNO_3$	Extracellular	10-20	Spherical	Antifungal	Gajbhiye *et al.* 2009
Hormoconis resinae	$AgNO_3$	Extracellular	20-80	Irregular	-	Varshney *et al.* 2009
Amylomyces rouxii strain KSU-09	$AgNO_3$	Extracellular	5-27	Spherical	Antimicrobial	Mussarat *et al.* 2010
Penicillium purpurogenum NPMF	$AgNO_3$	Extracellular	8–10	Spherical	Antimicrobial	Nayak *et al.* 2011
Humicola sp	$AgNO_3$	Extracellular	5–25	Spherical	-	Syed *et al.* 2013
Penicillium nalgiovense AJ12	$AgNO_3$	Extracellular	25.8±2.8	Spherical	-	Maliszewska *et al*. 2014
Rhizopus stolonifer	$AgNO_3$	Extracellular	54.67± 4.1	Irregular	-	AbdelRahim *et al*. 2017
Pleurotus ostreatus	$AgNO_3$	Extracellular	<40	Spherical	Antibacterial	Al-Bahrani *et al*. 2017
Penicillium spp	$AgNO_3$	Extracellular	149-397	Spherical	-	Verma *et al.* 2017

Fungi are exceptionally proficient secretors of extracellular enzymes which can be used for obtaining large-scale production of enzymes. Further advantages of using a fungal-mediated green approach for the synthesis of MNPs include economic viability and ease in handling biomass. Both intracellular and extracellular synthesis of MNPs can be carried out using fungi since they secrete enormous enzymes which can be used for the reduction of metal ion (Mandal *et al*. 2006).

Mukhergee *et al*. showed that the fungal biomass of *Verticillium sp*. resulted in the accumulation of AgNPs below the fungal cell surface when exposed to aqueous silver nitrate solution (Mukherjee *et al*. 2001). Chen *et al*. have shown that *Phoma sp.*3.2883 was, in fact, a biosorbent which was suited for preparing AgNPs (Chen *et al*. 2003). Vigneshwaran *et al*. also showed the accumulation of AgNPs with the average size 8.92 nm when incubated with silver nitrate solution for 72 hrs (Vigneshwaran *et al*. 2007). Ahmad *et al*. observed that when the aqueous Ag^+ are exposed to the *Fusarium oxysporum*, the Ag^+ get reduced by the enzymes and formed AgNPs in the range of 5-15 nm with high stability due to the protein secreted by a fungus (Ahmad *et al*. 2003b). Bhainsa and D'Souza reported the rapid extracellular synthesis of mono-dispersed AgNPs using *Aspergillus fumigatus* (Bhainsa and D'souza 2006). Duran *et al*. have reported the extracellular synthesis of AgNPs using *Fusarium oxysporum* (Durán *et al*. 2005). *Fusarium semitectum, Fusarium acuminatum*, and *Penicillium brevicompactum WA 2315* were also showed the potential towards the successful reduction of silver nitrate for the extracellular synthesis of AgNPs (Basavaraja *et al*. 2008, Ingle *et al*. 2008, Shaligram *et al*. 2009). Kathiresan *et al*. performed the in vitro synthesis of AgNPs where $AgNO_3$ was taken as a substrate and *Penicillium fellutanum* isolated from coastal mangrove sediment was taken as a source of enzyme (Kathiresan *et al*. 2009).

Gajbhiye *et al*. and Varshney *et al*. also reported the extracellular synthesis of AgNPs using *Alternaria alternate* and *Hormoconis resinae* respectively (Gajbhiye *et al*. 2009, Varshney *et al*. 2009). The eco-friendly optimized synthesis of AgNPs was carried out by Nayak *et al*. using *Penicillium purpurogenum* NPMF and observed the increased synthesis of AgNPs on increasing the concentration of silver nitrate. The effect of pH on the synthesis was also observed which affected the shape and size of the AgNPs (Nayak *et al*. 2011). A newly fungal strain *Amylomyces rouxii strain* KSU-09 isolated from the roots of date palm showed the synthesis of monodispersed spherical AgNPs (Mussarat *et al*. 2010). Syed *et al*. have shown the anticancerous activity of AgNPs prepared from *Humicola sp.* (Syed *et al*. 2013). Intracellular and extracellular synthesis of AgNPs using *Schizophyllum commune* were also investigated by Arun *et al*. which produced spherical AgNPs with average size 100 nm. Thus obtained AgNPs were further used in the biomedical application (Arun *et al*. 2014). Maliszewska *et al*. have used the cell free filtrate of *Penicillium nalgiovense* AJ12 for the extracellular synthesis of AgNPs (Maliszewska *et al*. 2014). Devi and Joshi have prepared spherical AgNPs with size ranging from 3.5 ± 3 nm using *Aspergillus niger PFR6, Penicillium ochrochloron PFR8, Potentilla fulgens L* (Devi and Joshi 2015). Recently, Singh *et al*., AbdelRahim *et al*., Al-Bahrani *et al*., and Verma *et al*. have reported the synthesis of AgNPs using *Rhizopus stolonifer*, *Pleurotus ostreatus*, and *Penicillium spp* respectively (AbdelRahim *et al*. 2017, Al-Bahrani *et al*. 2017, Verma *et al*. 2017) (**Table 1.3**).

Mukherjee *et al*. have demonstrated the use of eukaryotic microorganisms for the synthesis of AuNPs using *Verticillium sp*. (Mukherjee *et al*. 2001). Mukhergee *et al*. have investigated the green synthesis of AuNPs in 72 hrs using *Fusarium oxysporum* as a source

of reductases and obtained spherical AuNPs having size range 20-40 nm (Mukherjee *et al*. 2002).

Table 1.4 List of fungal stains used in the biosynthesis of AuNPs

Fungi	Precursor	Intracellular/ Extracellular	Size (nm)	Morphology	Application	Reference
Verticillium	$HAuCl_4$	Intracellular	10-15	Spherical	Antifungal	Mukherjee *et al.* 2001
Fusarium oxysporum	$HAuCl_4$	Extracellular	20-40	Spherical	-	Mukherjee *et al.* 2002
Rhodococcus sp	$HAuCl_4$	Intracellular	5-15	Spherical	-	Ahamad *et al*. 2003
Thermomonospora sp	$HAuCl_4$	Extracellular	8	Spherical	-	Ahamad *et al*. 2003
Trichothecium sp	$HAuCl_4$	Intracellular/Extracellular	-	Anisotropic	-	Ahmad *et al.* 2005
Volvariella volvacea	$HAuCl_4$	Extracellular	20-150	Triangular, Hexagonal	-	Philip 2009
Hormoconis resinae	$HAuCl_4$	Extracellular	3-20	Spherical	-	Mishra *et al.* 2010
Aspergillus oryzae	$HAuCl_4$	Extracellular	10-60	Spherical	-	Binupriya *et al.* 2010
Cylindrocladium floridanum	$HAuCl_4$	Extracellular	25	Spherical	-	Narayanan and Shakthivel, 2011
Epicoccum nigrum	$HAuCl_4$	Extracellular	5-50	Spherical	-	Sheikhloo *et al.* 2011
Neurospora crassa	$HAuCl_4$	Extracellular	32	Spherical	-	Castro- Longoria, *et al.* 2011
Penicillium brevicompactum	$HAuCl_4$	Extracellular	5–50	Spherical	Cytotoxic	Mishra *et al*. 2011
Verticillium luteoalbum	$HAuCl_4$	Intracellular	-	irregular	-	Gericke *et al*. 2011
Penicillium sp.	$HAuCl_4$	Extra/Intracellular	30-50, 50	Spherical	-	Du *et al*. 2011
Rhizopus oryzae	$HAuCl_4$		5-65	irregular	Catalytic	Das *et al*. 2012
Trichoderma sp	$HAuCl_4$	Extracellular	8	Spherical	Biocatalytic and Antimicrobial	Mishra *et al*. 2014
Fusarium solani	$HAuCl_4$	Extracellular	20-50	Spherical	-	Gopinath and Arumugam, 2014
Aspergillus sydowii	$HAuCl_4$	Extracellular	10	Spherical		Vala 2014
Penicillium aculeatum	$HAuCl_4$	Extracellular	60	Spherical	Scolicidal	Barabadi *et al.* 2017
Aspergillus sp. WL-Au	$HAuCl_4$	Extracellular	4-29	Spherical	Catalytic	Shen *et al.* 2017

Ahmad *et al*. have observed the formation of monodispersed spherical shaped AuNPs with an average size ranging from 5-15 nm on the cell wall and cytoplasmic membrane of *Rhodococcus sp*. *(*Ahmad *et al*. 2003c). *Thermomonospora* sp. was also investigated by Ahmad *et al*. for the extracellular synthesis of spherical AuNPs with average size 8 nm (Ahmad *et al*. 2003a). Ahmad *et al*. have also investigated the intra and extracellular synthesis of AuNPs using *Trichothecium sp* (Ahmad *et al*. 2005). Gericke and Pinches have successfully demonstrated an intracellular as well as the extracellular synthesis of AuNPs in the presence of *Verticillium luteoalbum* extract (Gericke and Pinches 2006b). Du *et al*. have reported the both extracellular (30-50 nm) and intracellular (50 nm) synthesis of spherical AuNPs from *Penicillium sp*. (Du *et al*. 2011). A simple one-pot green method was used by Das *et al*. for the synthesis of AuNPs with the size ranged from 5-65 nm using protein extract of *Rhizopus oryzae* (Das *et al*. 2012). Mishra *et al*. have also reported the green synthesis of anisotropic AuNPs of size ranging from 3-20 nm using *Hormoconis resinae* (Mishra *et al*. 2010). The supernatant, live cell filtrate and biomass of the fungus *Penicillium brevicompactum* were applied for the synthesis of AuNPs by Mishra *et al*. group for the cytotoxic study against mouse mayo blast cancer C_2C_{12} cells (Mishra *et al*. 2011). Mishra *et al*. have also investigated the synthesis of AuNPs from the *Trichoderma sp*. for the biocatalytic and antimicrobial activity (Mishra *et al*. 2014). Gopinath and Arumugam have used culture extract of *Fusarium solani* for the synthesis of AuNPs (Gopinath and Arumugam 2014). Vala has synthesized AuNPs using a marine-derived fungus *Aspergillus sydowii* (Vala 2015). *Cylindrocladium floridanum* also showed its potential towards the successful extracellular synthesis of spherical AuNPs with average size 25 nm (Narayanan and Sakthivel 2011). *Aspergillus oryzae* was also investigated for its potential towards the

extracellular synthesis of AuNPs which showed that the synthesized AuNPs were spherical in shape with size ranging from 10-60 nm (Binupriya *et al*. 2010). Sheikhloo *et al*. have reported the green synthesis of AuNPs using *Epicoccum nigrum* (Sheikhloo *et al*. 2011). Castro- Longoria, *et al*. have shown the synthesis of AuNPs with 32 nm of size from using filamentous fungi *Neurospora crassa* (Castro-Longoria *et al*. 2011). Recently, Barabadi *et al*. have showed the preparation of AuNPs with an average size 60 nm using *Penicillium aculeatum* to investigate the scolicidal activity (Barabadi *et al*. 2017). Shen *et al*. have also investigated the extracellular synthesis of AuNPs using Aspergillus sp. WL-Au for the catalytic reduction of 4-nitrophenol (Shen *et al*. 2017) (**Table 1.4**).

1.4.1.3 Algae

The phyco-mediated green synthesis of AgNPs and AuNPs has also become one of the prominent areas of research in nanoscience and nanotechnology. Algae are also being extensively used as a factory for the green synthesis of AgNPs and AuNPs. Several important phytochemicals required for the reduction of metal ions are present in the algae which play very important role in the reduction as well as stabilization process. These phyto-chemicals include hydroxyl, carboxyl and amino functional groups which can serve both as effective metal-reducing agents as well as capping agents. Due to the presence of these chemicals, algae can synthesize the nanoparticles by intra and extracellular manner.

Barwal *et al*. have exploited the unicellular algae *Chlamydomonas reinhardtii* as a model system to elucidate the role of cellular proteins in intra and extracellular synthesis of AgNPs. They observed that the cytoplasm was filled with the AgNPs (Barwal *et al*. 2011). The intra and extracellular synthesis of AgNPs were also performed by Jena *et al*. by using *Chlorococcum humicola* and obtained spherical AgNPs with a size range of 4-16 nm (Jena *et*

al. 2013). Kanan *et al*. have demonstrated the intracellular synthesis of AgNPs with average size 30 nm using the extract of *Chaetomorpha linum* by the reduction of the aqueous silver metal ions (Kannan *et al*. 2013).

Table 1.5 List of algal strains used in the biosynthesis of AgNPs

Algae	Precursor	Intracellular /Extracellular	Size (nm)	Morphology	Application	Reference
Chlamydomonas reinhardtii	$AgNO_3$	Intracellular/ Extracellular	5-15 & 5-35	Spherical	-	Barwal *et al.* 2001
Chlorococcum humicola	$AgNO_3$	Intracellular/ Extracellular	4-16	Spherical	Antibacterial	Jena *et al*. 2012
Chaetomorpha linum	$AgNO_3$	Intracellular	3-44	Clustres	-	Kanan *et al.* 2013
Leptolyngbya valderianum	$AgNO_3$	Intracellular	2-20	Spherical	-	Roychoudhury and Pal 2014
Caulerpa racemosa	$AgNO_3$	Intracellular/ Extracellular	05–25	Spherical & Triangular	Antibacterial	Kathiraven *et al.* 2015
Turbinaria conoides	$AgNO_3$	Extracellular	5-50	Spherical	Fabric strengthening	Sheeba and Thambidurai 2009
Sargassum Wightii Grevill	$AgNO_3$	Extracellular	8-27	Spherical	-	Govindaraju *et al*. 2009
Ulva lactuca	$AgNO_3$	Extracellular	48.59	Spherical	Catalytic	Kumar *et al.* 2011
Sargassum tenerrimum	$AgNO_3$	Extracellular	20	Spherical	Antibacterial	Kumar *et al.* 2012
Turbinaria conoides	$AgNO_3$	Extracellular	96	Spherical	Antibacterial	Rajeshkumar *et al*. 2012
Cystophora moniliformis	$AgNO_3$	Extracellular	5-100	Spherical	-	Prasad *et al.* 2013
Sargassum longifolium	$AgNO_3$	Extracellular	5–50	Spherical, Ellipsoidal	Antifungal	Rajeshkumar *et al*. 2014
Pithophora oedogonia	$AgNO_3$	Extracellular	34.03	Irregular	-	Sinha *et al*. 2014
Sargassum plagiophyllum	$AgNO_3$	Extracellular	18-42	Spherical	Antibacterial	Dhas *et al* 2014
Ulva flexousa	$AgNO_3$	Extracellular	2-32	irregular	-	Rahimi *et al.* 2014
Hypnea musciformis	$AgNO_3$	Extracellular	40-65	Spherical	Mosquitocidal, Pesticidal	Roni *et al*. 2015
Centroceras clavulatum	$AgNO_3$	Extracellular	35-65	Spherical	Mosquitocidal activity	Murugan *et al.* 2016
Spirogyra varians	$AgNO_3$	Extracellular	17.6	Anisotropic	Antibacterial	Salari *et al.* 2016
Caulerpa serrulata	$AgNO_3$	Extracellular	10±2	Spherical	Catalytic, Antibacterial	Aboelfetoh *et al.* 2017

The intracellular synthesis of AgNPs was also carried out by Roychoudhury and Pal by exposing the healthy biomass of *Leptolyngbya valderianum* to the 100 mL of 9 mM aqueous silver metal ion solution for 72 hrs (Roychoudhury and Pal 2014). Recently, Kathiraven *et al*. have presented green synthesis and antibacterial activity of AgNPs using *Caulerpa racemosa*, a marine alga, collected from the Gulf of Mannar (Kathiraven *et al*. 2015). Sheeba and Thambidurai, have shown the extracellular synthesis of AgNPs with the size range from 5-50 nm using *Turbinaria conoides* (Sheeba and Thambidurai 2009). Similarly, *Sargassum wightii* was exploited for the synthesis of AgNPs by Govindaraju *et al*. (Govindaraju *et al*. 2009). Kumar *et al*. have used *Ulva lactuca* and synthesized spherical AgNPs with average size 48.59 nm for the catalytic degradation of methyl orange (Kumar *et al*. 2013). Kumar *et al*. have also corroborated the eco-friendly extracellular synthesis of AgNPs using the extract of *Sargassum tenerrimum* for the antibacterial activity (Kumar *et al*. 2012a). *Turbinaria conoides* (Rajeshkumar *et al*. 2012) *Cystophora moniliformis* (Prasad *et al*. 2013), *Sargassum longifolium* (Rajeshkumar *et al*. 2014), *Pithophora oedogonia* (Sinha *et al*. 2015), *Colpomenia sinuosa* (Vishnu Kiran and Murugesan 2014), *Sargassum plagiophyllum* (Dhas *et al*. 2014, Rahimi *et al*. 2014a), and *Ulva flexousa* (Rahimi *et al*. 2014b) were also used for the extracellular synthesis of AgNPs for various applications. The extracellular synthesis of AgNPs was also demonstrated by Roni *et al*. using the extract of *Hypnea musciformis* and utilized the prepared AgNPs in mosquitocidal and pesticidal activity (Roni *et al*. 2015). Madhiyazhagan *et al*. have shown the green synthesis of AgNPs having size 43-79 nm using *Sargassum muticum* and investigated the antibacterial and larvicidal activity (Madhiyazhagan *et al*. 2015). Recently, Murugan *et al*. have used the extract of *Centroceras clavulatum* for the extracellular synthesis of AgNPs and applied it for the mosquitocidal activity (Murugan

et al. 2016). Similarly, Salari *et al*. have also synthesized AgNPs having the size 17.6 nm using *Spirogyra varians* for the antibacterial activity (Salari *et al*. 2016). Recently, Aboelfetoh *et al*. have reported the green and eco-friendly synthesis of AgNPs using *Caulerpa serrulata*, a green alga. They observed that the synthesized AgNPs were spherical shaped with the average size 10±2 nm which were further investigated against the catalytic degradation of azo dye and antibacterial activity against both Gram-negative bacteria (*Escherichia coli*, *Staphylococcus aureus*, *Shigella sp*., and *Salmonella typhi*) and Gram-positive bacteria (*Pseudomonas aeruginosa*) (Aboelfetoh *et al*. 2017) (**Table 1.5**).

The synthesis of the nanoparticles is affected by many parameters such as temperature, pH, metal ion concentration, stirring and static conditions etc. It is believed the metal ions are reduced by the enzymes secreted by an algal cell which is followed by nucleation and growth. The intracellular synthesis mainly depends on physico-chemical parameters like temperature, pH, and concentration of the metal ions. The surface-bound proteins and their residual amino acids viz cysteine, tyrosine, and tryptophan play a vital role though amine (NH_2) groups in capping and stabilization of nanoparticles at basic pH.

Hosea *et al*. have investigated the effect of parameters influencing the accumulation of Au(0) on the alga *Chlorella vulgaris*. They have also examined the rate and extent of reduction of algal-bound Au (I) and found that the amount of algal-bound atomic gold produced from ionic gold increased with time (Hosea *et al*. 1986). Konishi *et al*. reported the intracellular synthesis of AuNPs in size range of 15-200 nm using *Shewanella sps*. (Konishi *et al*. 2006). Senapati *et al*. also demonstrated the intracellular synthesis of spherical AuNPs having a size range from 5-35 nm utilizing *Tetraselmis kochinensis* (Senapati *et al*. 2012).

Table 1.6 List of algal strains used in the biosynthesis of AuNPs

Algae	Precursor	Intracellular/ Extracellular	Size (nm)	Morphology	Application	Reference
Chlorella vulgaris	$HAuCl_4$	Intracellular	-	Spherical	Irregular	Hosea *et al*. 1986
Shewanella sps.	$HAuCl_4$	Intracellular	15-200	Spherical	-	Konishi *et al*. 2007
Tetraselmis kochinensis	$HAuCl_4$	Intracellular	5-35	Spherical	-	Senapati *et al.* 2012
Chlorella vulgaris	$HAuCl_4$	Extracellular	-	Triangular, Hexagon	-	Xie *et al*. 2007
Fucus vesiculosus	$HAuCl_4$	Extracellular	-	Anisoptropic	-	Mata *et al*. 2009
Laminaria japonica	$HAuCl_4$	Extracellular	15-20	Spherical	-	Ghodake and Lee, 2011
Stoechospermum marginatum	$HAuCl_4$	Extracellular	18.7-93.7	Irregular	Antibacterial	Rajathi *et al.* 2012
Klebsormidium flaccidum	$HAuCl_4$	Extracellular	8.6±4.2	Spherical	-	Dahaumane *et al.* 2012
Chlorella pyrenoidusa	$HAuCl_4$	Extracellular	25-30	Irregular	-	Oza *et al*. 2012
Spirulina platensis	$HAuCl_4$	Extracellular	12	Irregular	-	Mahdieh *et al.* 2012
Padina gymnospora	$HAuCl_4$	Extracellular	53-67	Irregular		Singh *et al*. 2013
Turbinaria conoides	$HAuCl_4$	Extracellular	60	Irregular	Antibacterial	Rajeshkumar *et al*. 2013
Ecklonia cava	$HAuCl_4$	Extracellular	20-50	Spherical	Antibacterial	Venkatesan *et al.* 2014
Spirogyra submaxima	$HAuCl_4$	Extracellular	2-50	Spherical, Hexagonal	-	Roychoudhury and Pal, 2014
Lemanea fluviatilis	$HAuCl_4$	Extracellular	5-15	Spherical	Antioxidant	Sharma *et al.* 2014
Turbinaria conoides	$HAuCl_4$	Extracellular	17.6±0.42	Spherical	-	Vijayan *et al.* 2014
Chlorella vulgaris	$HAuCl_4$	Extracellular	2-10	Spherical	Antipathogenic	Annamalai and Nallamuthu, 2015
Padina pavonica	$HAuCl_4$	Extracellular	30-70	Irregular	Antibacterial	Isaac *et al*. 2015
Rhizoclonium fontinale	$HAuCl_4$	Extracellular	16	Spherical	-	Parial *et al*. 2015
Cystoseira baccata	$HAuCl_4$	Extracellular	8.4±2.22	Spherical	Anticancerous	Gonzalez-Ballestero *et al.* 2017

Recently, Dahoumane *et al*. have studied that the process of biomineralization occurs within the thylakoidal membranes where the available enzymes reduce the gold metal ions for the formation of AuNPs (Dahoumane *et al*. 2012). Xie *et al*. have reported the extracellular

synthesis of triangular and hexagonal AuNPs using *Chlorella vulgaris* (Xie *et al*. 2007) Similarly, Mata *et al*. 2009 investigated the synthesis of anisotropic AuNPs using *Fucus vesiculosus* (Mata *et al*. 2009). Ghodake and Lee have exploited *Laminaria japonica* to synthesize AuNPs having size 15-20 nm (Ghodake and Lee 2011). *Stoechospermum marginatum* (Rajathi *et al*. 2012), *Klebsormidium flaccidum*, (Dahoumane *et al*. 2012) *Chlorella pyrenoidusa* (Oza *et al*. 2012) (Oza *et al*. 2012) and *Spirulina platensis* (Mahdieh *et al*. 2012) have been used for the extracellular synthesis of AuNPs. *Padina gymnospora* and *Turbinaria conoides* have been utilized for the extracellular synthesis of AuNPs by Singh *et al*. and Rajeshkumar *et al*. respectively (Singh *et al*. 2013, Rajeshkumar *et al*. 2013). Venkatesan *et al*. have performed the antibacterial activity using AuNPs synthesized from *Ecklonia cava* (Venkatesan *et al*. 2014). Roychoudhury and Pal have synthesized AuNPs using extracellular pathway from a unicellular alga *Spirogyra submaxima* (Roychoudhury and Pal 2014). *Lemanea fluviatilis* and *Turbinaria conoides* have also been exploited to obtain AuNPs extracellularly (Sharma *et al*. 2014, Vijayan *et al*. 2014). Annamalai and Nallamuthu have used *Chlorella vulgaris* to obtain spherical AuNPs within 2-10 nm for antibacterial activity (Annamalai and Nallamuthu 2015). Isaac *et al*. 2015 have also investigated the antibacterial activity of irregular AuNPs (30-70 nm) synthesized from *Padina pavonica* (Isaac and Renitta 2015). Recently, Gonzalez-Ballestero *et al*. 2017 have investigated the anticancerous activity of AuNPs on colon cancer cell lines HT-29 and Caco-2, as well as on normal primary neonatal dermal fibroblast cell line PCS-201-010 which was synthesized from *Cystoseira baccata* (González-Ballesteros *et al*. 2017) which is given in Table 1.6.

1.4.1.4 Actinomycetes and Yeast

Actinomycetes are commonly known as ray fungi and regarded as the primary source for the synthesizing secondary metabolites like antibiotics in general. They are the rich source of the potent enzymes and hence can be utilized for the synthesis of nanoparticles. In this connection, Ahamad *et al*. have reported the intracellular synthesis of AuNPs with a dimension of 5–15 nm using an alkalotolerant actinomycete, *Rhodococcus sp.* and observed that the AuNPs were accumulated on the cell wall and cytoplasmic membrane with good dispersity. The enzyme reductase present in cell wall and the cytoplasmic membrane were chief reducing agent for the reduction of Au^{3+} to Au^{0} (Ahmad *et al*. 2003a) Ahamad *et al*. 2003 have also reported the extracellular synthesis of AuNPs using a novel extremophilic actinomycete, *Thermomonospora sp.* which was potent enough to synthesize extracellular monodispersed spherical AuNPs with an average size of 8 nm (Ahmad *et al*. 2003a). Alani *et al*. have investigated the extracellular synthesis of AgNPs having size 15-45 nm using a *Streptomyces sp* (Alani *et al*. 2012). *Streptomyces albidoflavus,* an actinomycete was utilized against the extracellular formation of spherical AgNPs using its extract (Prakasham *et al*. 2012). Similarly, Manivasagan *et al*. have also reported the AuNPs formation from *Nocardiopsis sp.* MBRC-1 (Manivasagan *et al*. 2013). Similarly, Otari *et al*., Chauhan *et al*., Thenmozhi *et al*., Manikprabhu *et al*., and Subashini and Kannabiran have also reported the synthesis of AgNPs using Rhodococcus sp., Streptomyces sp JAR1, Streptomyces sp. VITSTK7, *Streptomyces sp*. and Streptomyces sp. VITBT7 respectively (Otari *et al*. 2012, Chauhan *et al*. 2013, Thenmozhi *et al*. 2013, Manikprabhu and Lingappa 2013, Subashini and Kannabiran 2013).

Table 1.7 List of actinomycetes and yeasts used in the biosynthesis of AgNPs and AuNPs

Actinomycetes	Precursor	Intracellular/ Extracellular	Size (nm)	Morphology	Application	Reference
Rhodococcus sp.	$HAuCl_4$	Intracellular	5-15	Irregular	-	Ahamad *et al*. 2003
Thermomonospora sp	$HAuCl_4$	Extracellular	8-40	Spherical	-	Ahamad *et al*. 2003
Streptomyces sp. NK52	$HAuCl_4$	Extracellular	10-100	Anisotropic	Antilipid peroxidation activity	Prakash *et al*. 2013
Streptomyces sp	$AgNO_3$	Extracellular	15-25	Spherical		Alani *et al.* 2012
Streptomyces albidoflavus	$AgNO_3$	Extracellular	10-40	Irregular	Antibacterial	Prakasham *et al*. 2012
Actinomycetes sp	$AgNO_3$	Extracellular	40-63	Spherical	Antibacterial	Sunitha *et al.* 2013
Nocardiopsis sp	$AgNO_3$	Extracellular	30-90	Irregular	Antimicrobial and cytotoxic	Manivasagan *et al*. 2013
Rhodococcus sp.	$AgNO_3$	Extracellular	10	Spherical	-	Otari *et al.* 2012
Streptomyces sp JAR1	$AgNO_3$	Extracellular	68.13	Irregular	Antibacterial	Chauhan *et al*. 2013
Streptomyces sp. VITSTK7	$AgNO_3$	Extracellular	20-60	Irregular	Antifungal	Thenmozhi *et al*. 2013
Streptomyces s p	$AgNO_3$	Extracellular	28-50	Irregular	Antibacterial	Manikprabhu *et al*. 2013
Streptomyces sp. VITBT7	$AgNO_3$	Extracellular	20–70	Irregular	Antibacterial and Antifungal	Subashini and Kannabiran,2013
Streptacidiphilus durhamensis	$AgNO_3$	Extracellular	8-48	Irregular	Antibacterial	Buszewski *et al.* 2016
Gordonia amicalis HS-11	$AgNO_3$	Extracellular	5-25	Spherical	Antioxidant	Sowani *et al*. 2016
Yeast						
Saccharomyces cerevisiae	$HAuCl_4$	Extracellular	-	Irregular	-	Lin *et al*. 2005
Pichia jadinii	$HAuCl_4$	Intracellular	100	Anisotropic	-	Gericke *et al*. 2006
Yarrowia lipolytica NCIM 3589	$HAuCl_4$	Intracellular	15	Trigonal, Hexagonal	-	Agnihotri *et al*. 2009
Yeast MKY3	$HAuCl_4$	Extracellular	2-5	Spherical	-	Kowshik *et al.* 2002
Yeast extract	$HAuCl_4$	Extracellular	1300 ±200	Hexagonal	-	Yang *et al.* 2017

Recently, Sowani *et al*. have shown the extracellular green synthesis of both AgNPs and AuNPs with a size range of 5-25 nm (Sowani *et al*. 2016). Buszewski *et al*. have also reported the synthesis of AgNPs using in size range from 8-48 nm and investigated antibacterial activity (Buszewski *et al*. 2016).

Among the eukaryotic microorganism, yeast has been exploited mainly for the synthesis of semiconductors but, few of them were also reported for the synthesis of AgNPs and AuNPs. *S. cerevisiae* was reported to biosorb and reduces Au^{+3} to elemental gold on the peptidoglycan layer of the cell wall by the aldehyde group present in reducing sugars (Lin *et al*. 2005). Similarly, Gericke and Pinches have shown the intracellular synthesis of spherical, triangular and hexagonal AuNPs using *Pichia jadinii* (Gericke and Pinches 2006a). Agnihotri *et al*. have studied the pH-dependent synthesis of AuNPs using *Yarrowia lipolytica* NCIM 3589. They observed that the reduction of gold ions occurred in pH dependent manner. When cells were incubated at pH 2.0, hexagonal and triangular AuNPs were formed due to the nucleation on the cell surfaces which produced golden color in the visible region at 540 nm. Whereas, at pH 7.0 and pH 9.0, it produced pink and purple colors respectively having an average size 15 nm (Agnihotri *et al*. 2009). The yeast MKY3 is a silver tolerant strain and reported for the extracellular synthesis of hexagonal AgNPs (Kowshik *et al*. 2002) (**Table 1.7**).

1.4.2 Plants

Since last decades, the plant extracts have been used as a great source of reducing and stabilizing agent for the eco-friendly, economically viable and rapid synthesis of stable AgNPs and AuNPs. The plants contain several phytochemicals such as tannins, flavonoids, proteins, amino acids, enzymes, polysaccharides, alkaloids, terpenoids, triterpenoids,

phenolics, saponins, etc. which act as a potential reducing and stabilizing agent. Therefore, plants have been found a most suitable resource for the synthesis of AgNPs and AuNPs. The AgNPs and AuNPs synthesized by plant extract have been proved to be more advantageous regarding biocompatibility, scalability, and the medical applicability than chemically synthesized nanoparticles. Therefore, the plants are most preferred for the synthesis of AgNPs and AuNPs.

The first report on the plant-mediated synthesis of metal nanoparticles was presented by Gardea-Torresdey *et al*. using *Alfalfa* sprouts (Gardea-Torresdey *et al*. 2002). Thereafter, several reports on the synthesis of AgNPs and AuNPs and their potential applications have been published by plant leaf extracts which are given in **Table 1.8** (Chandran *et al*. 2006, Sathishkumar *et al*. 2009, Raut *et al*. 2010, Bar *et al*. 2009, Parashar *et al*. 2009, Jha *et al*. 2009, Kesharwani *et a*l. 2009, Ahmad *et al*. 2010a, Elumalai *et al*. 2010, Ravindra *et al*. 2010, Roy and Barik 2010, Bankar *et al*. 2010, Saxena *et al*. 2010, Dwivedi and Gopal 2010, Philip 2010a, b, Prasad and Elumalai 2011, Philip *et al*. 2011, Veerasamy *et al*. 2011, Prathna *et al*. 2011, Vidhu *et al*. 2011, Santhoshkumar *et al*. 2011, Mondal *et al*. 2011, Sivakumar *et al*. 2012, Von White *et al*. 2012, Vijayaraghavan *et al*. 2012, Gopinath *et al*. 2012, Umadevi *et al*. 2013, Mude *et al*. 2009, Arunkumar *et al*. 2013, Rodríguez-León *et al*. 2013, Ahmad *et al*. 2010b, Kudle *et al*. 2012, Parvathy *et al*. 2014, Awad *et al*. 2014, Praba *et al*. 2014, Kudle *et al*. 2014, Mohamed *et al*. 2014, Nakkala *et al*. 2014, Arokiyaraj *et al*. 2014, Shetty *et al*. 2014, Paulkumar *et al*. 2014, Baharara *et al*. 2014, Kathiravan *et al*. 2014, Narayanan and Park 2014, Subbaiya *et al*. 2014, Shams *et al*. 2014, Rahimi-Nasrabadi *et al*. 2014, Korbekandi *et al*. 2015, Rajagopal *et al*. 2015, Paul *et al*. 2015a, Raja *et al*. 2015, Sadeghi and Gholamhoseinpoor 2015, Yang *et al*. 2015, Ali *et al*. 2015, Ashour *et al*. 2015, Suresh *et*

al. 2015, Shalaby *et al*. 2015, Padalia *et al*. 2015, Heydari and Rashidipour 2015, Billacura and Mimbesa 2015). Ahmad *et al*. have investigated the antibacterial and photoluminescence activity of AgNPs synthesized by *Azadirachta indica* (Ahmed *et al*. 2016a). The bark extract of *Terminalia arjuna* was also investigated by Ahmad *et al* towards the green synthesis of AgNPs and obtained spherical AgNPs in the range of 2-100 nm (Ahmed *et al*. 2016b). Al-Shmgani *et al*., Saravanakumar *et al*. and Bhuvaneswari *et al*. have utilized the leaf extracts of *Catharanthus roseus*, *Prunus japonica*, and *Excoecaria agallocha* respectively for the synthesis of AgNPs. The AgNPs synthesized by *Catharanthus roseus* were spherical in shape with the average size 20 nm whereas the AgNPs obtained by *Prunus japonica* were different shape like hexagona, trigonal, and spherical with the average size 26 nm. The AgNPs obtained from *Excoecaria agallocha* were also of different shape like hexagonal and spherical which showed potent antibacterial and antioxidant activity (Al-Shmgani *et al*. 2016, Saravanakumar *et al*. 2016, Bhuvaneswari *et al*. 2017). Ravichandran *et al*. 2016 have synthesized spherical AgNPs using *Artocarpus altilis* with the average size 38 nm and performed the antimicrobial and antioxidant activity (Ravichandran *et al*. 2016). The AgNPs synthesized by *Terminalia cuneata* showed excellent catalytic activity (Edison *et al*. 2016). Nayak *et al*. 2016 have performed the synthesis of spherical AgNPs using *Ficus benghalensis* and investigated the antibacterial and Antiproliferative activity (Nayak *et al*. 2016). The leaf extract of *Phoenix Dactylifera* was to synthesize the AgNPs. The results indicated the synthesis of irregular shaped AgNPs with size range 20-60 nm which showed the catalytic activity (Aitenneite *et al*. 2016). The fruit and leaf extracts of *Capuli cherry* and *Mussaenda glabrata* were also utilized for the green synthesis of AgNPs. The results revealed the presence of spherical AgNPs in the size range of 20-80 nm and 51.32 nm respectively

(Francis *et al*. 2017, Kumar *et al*. 2016a). Similary, several authors have reported the green synthesis of AgNPs using different parts of the plants and utilized in various applications (Mohammadi *et al*. 2016, Ali *et al*. 2016a, Ali *et al*. 2016b, Ramachandran *et al*. 2016, Mosae Selvakumar *et al*. 2016, Sánchez *et al*. 2016, Lakshman Kumar *et al*. 2016, Verma *et al*. 2016, Ajitha *et al*. 2016, Kumar *et al*. 2016b, Anandalakshmi *et al*. 2016, Karunakaran *et al*. 2016, Velayutham *et al*. 2016, Bharathi *et al*. 2016, Begum *et al*. 2016, Kumar *et al*. 2017a, Chaudhuri *et al*. 2016, Dong *et al*. 2016)

Recently, Devanesan *et al*. have synthesized the AgNPs using the seed extracts of *Pimpinella anisum*. The synthesized AgNPs (80-85 nm) were further investigated for their cytotoxic effect on colorectal cancer (CRC) cell lines. Thus obtained AgNPs showed the potent cytotoxic effect on colorectal adenocarcinoma CRC cells. The results indicated that the cancerous cells were killed selectively through the arrest of cell cycle at the G2/M phase, suppression of proliferation, and apoptosis induction (Devanesan *et al*. 2017). Silva-De Hoyos *et al*. have prepared the spherical AgNPs with average size 7 nm using the aqueous leaf extract of *Camella sinesis*. The synthesized AgNPs were further used for the sensing of Cu^{2+} and Pb^{2+} (Silva-De Hoyos (Silva-De Hoyos *et al*. 2017). Kasithevar *et al*. also used the leaf extract of Alysicarpus monilifer. They observed that the AgNPs synthesized were spherical with average 15 ± 2 nm and showed potent antibacterial activity (Kasithevar *et al*. 2017). The fruit extract of tamarind was employed for the synthesis of AgNPs and found that the synthesized AgNPs were spherical with average size 10 nm which showed excellent results towards the antibacterial activity (Jayaprakash *et al*. 2017). The irregular shaped AgNPs with average size 37.86 nm was synthesized by Francis *et al*. using the leaf extract of *Elephantopus scaber* and also investigated its antibacterial activity (Francis *et al*. 2017).

Other parts of the different plants were also used widely for the synthesis of AgNPs because of their great potential to act as reducing and stabilizing agent. For example, the rhizome of turmeric was utilized by Nayak *et al.* for the synthesis of AgNPs in size range of 120-160 nm which was also used for the investigation of antibacterial activity (Nayak *et al.* 2017).

Table 1.8 List of different plants and their parts used in the biosynthesis of AgNPs.

Plants	Precursor	Parts of the plant	Size (nm)	Morphology	Application	Reference
Alfalfa	$AgNO_3$	Sprout	2-4	Spherical	-	Gardea-Torresdey *et al.* 2003
Aloe vera	$AgNO_3$	Leaf	15.2 nm ± 4.2 nm	Spherical	-	Chandran *et al.* 2006
Cinnamon zeylanicum	$AgNO_3$	Bark extract	31-40	Cubic, Hexagonal	-	Sathishkumar *et al.* 2009
Gliricidia sepium	$AgNO_3$	Leaf	10-50	Spherical	Antibacterial	Raut *et al.* 2010
Jatropha curcas	$AgNO_3$	Latex	10-20	Spherical	-	Bar *et al.* 2009
Mentha piperita	$AgNO_3$	Leaf	5-30	Spherical	-	Prasar *et al.* 2009
Parthenium hysterophorus	$AgNO_3$	Leaf	50	Irregular	-	Parashar *et al.* 2009
Cyperus sp.	$AgNO_3$	Leaf	2-5	Spherical	-	Jha *et al.* 2009
Datura metel	$AgNO_3$	Leaf	16-40	Spherical, Ellipsoidal	-	Kesharwani *et al.* 2009
Desmodium triflorum	$AgNO_3$	Leaf	5-20	Spherical	-	Ahmad *et al.* 2010
Euphorbia hirta	$AgNO_3$	Leaf	40-50	Irregular	Antibacterial	Elumalai *et al.* 2010
Ficus bengalensis	$AgNO_3$	Leaf	20	Spherical	Antibacterial	Ravindra *et al.* 2010
Ludwigia adscendens	$AgNO_3$	Leaf	100-400	Spherical	Antibacterial	Roy *et al.* 2010
Musa paradisiacal	$AgNO_3$	Peel	20	Spherical	Antibacterial and Antifungal	Bankar *et al.* 2010
Allium cepa	$AgNO_3$	Peel	33.6	Spherical	Antibacterial	Saxena *et al.* 2010
Pongam pinnata L. Pierre	$AgNO_3$	Leaf	38	Spherical	Antibacterial	Raut *et al.* 2010
Ocimum sanctum	$AgNO_3$	Root	10±2	Spherical	-	Ahmad *et al.* 2010
Chenopodium album	$AgNO_3$	Leaf	10-30	Quasi spherical	-	Dwivedi and Gopal 2010
Hibiscusrosa sinensis	$AgNO_3$	Leaf	14	Prism or Spherical	-	Philip *et al.* 2010
Moringa oleifera	$AgNO_3$	Leaf	57	Spherical	Antimicrobial	Prasad *et al.* 2011
Murraya koenigii	$AgNO_3$	Leaf	10	Spherical	-	Philip *et al.* 2011
Garcinia	$AgNO_3$	Leaf	35	Spherical	Antibacterial	Veerasamy *et al.* 2011

mangostana						
Citrus limon	$AgNO_3$	Juice	≤50	Spherical	-	Prathna *et al.* 2011
Macrotyloma uniflorum	$AgNO_3$	Leaf	12	Anisotropic		Vidhu *et al*. 2011
Nelumbo nucifera	$AgNO_3$	Leaf	25-80	Hexagonal	Larvicidal	Santhoshkumar *et al*. 2011
Swietenia mahogany	$AgNO_3$	Leaf	50	-	-	Mondal *et al.* 2011
Lantana camara	$AgNO_3$	Fruit	12.55–12.99	Spherical	Antibacterial	Sivakumar *et al.* 2012
Cuminum cyminum	$AgNO_3$	Seed	12	Spherical	-	Kudle *et al*. 2012
Garlic	$AgNO_3$	Peel	4-6	-	Cytotoxic	Von White *et al*. 2012
Trachyspermum ammi	$AgNO_3$	Seed	87	Irregular	-	Vijayaraghavan *et al.* 2012
Papaver somniferum	$AgNO_3$	Seed	99.8	Irregular	-	Vijayaraghavan *et al.* 2012
Tribulus terrestris	$AgNO_3$	Fruit	16–28	Spherical	Antibacterial	Gopinath *et al*. 2012
Solanum lycopersicum	$AgNO_3$	Fruit	10	Spherical	-	Umadevi *et al.* 2013
Carica papaya	$AgNO_3$	callus	60-80	Spherical	-	Mude Namrata *et al*. 2013
Tecoma stans	$AgNO_3$	Leaf	15	Spherical	-	Arunkumar *et al*. 2013
Rumex hymenosepalus	$AgNO_3$	Root	2-40	Hexagonal	-	Rodrıguez-Leon *et al.* 2013
Solanum nigrum	$AgNO_3$	Leaf	50-100	Spherical	Larvaecidal, Antimicrobial	Rawani, *et al.* 2013
Albizia lebbeck	$AgNO_3$	Leaf	-	Roughly Spherical	Antibacterial	Parvathy *et al*. 2014
Orange	$AgNO_3$	Peel	91	Spherical	Antibacterial	Awad *et al.* 2014
Piper betle	$AgNO_3$	Leaf	-	-	Antibacterial	Prabha *et al.* 2014
Justica adhatoda	$AgNO_3$	Leaf	11–20	Spherical	Cytotoxic, Antibacteria	Kudle *et al*. 2014
Calotropis procera	$AgNO_3$	Latex serum	12.33	Spherical	Antimicrobial	Mohamed *et al*. 2014
Alternanthera dentate	$AgNO_3$	Leaf	50–100	Spherical	-	Nakkala *et al*. 2014
Chrysanthemum indicum L	$AgNO_3$	Flower	37.71–71.99	Spherical	Antibacterial	Arokiyaraj *et al.* 2014
Alstonia scholaris	$AgNO_3$	Bark	50	Spherical	Antimicrobial	Shetty *et al.* 2014
Piper nigrum	$AgNO_3$	Leaf	7–50 and 9–30	Spherical	-	Paulkumar *et al.* 2014
Achillea bieberstennii	$AgNO_3$	Leaf	12 ± 2	Hexagonal, Pentagonal and Spherical	Anti-Angiogenic	Baharara *et al.* 2014
Melia dubia	$AgNO_3$	Leaf	35	Spherical	Cytotoxic	Kathiravan *et al*. 2014
Brassica rapa	$AgNO_3$	Leaf	16.4	Spherical	Antifungal	Narayanan *et al.* 2014
Nerium oleander	$AgNO_3$	Leaf	380–420	-	Antibacterial, Antoxidant	Subbaiya *et al*. 2014
Melia azedarach	$AgNO_3$	Seed	-	-	-	Shams *et al*. 2014

Eucalyptus leucoxylon	$AgNO_3$	Leaf	50	Spherical	Antioxidant	Rahimi-Nasrabadi *et al.* 2014
Quercus brantii	$AgNO_3$	Leaf	6	Polydispersed and Spherical	-	Korbekandi *et al.* 2015
Catharanthus roseus	$AgNO_3$	Leaf	35–55	Spherical	Larvicidal	Rajagopal *et al.* 2015
Premna serratifolia L.	$AgNO_3$	Leaf	22.97	Spherical	Cytotoxic	Paul *et al.* 2015
Calliandra haematocephala	$AgNO_3$	Leaf	70	Spherical	Antibacterial, H_2O_2 Detection	Raja *et al.* 2015
Ziziphora tenuior	$AgNO_3$	Leaf	8–40	Spherical	-	Sadeghi and Gholamhoseinpoor, 2015
Peach gum	$AgNO_3$	Peach gum Powder	23.56 ± 7.87	Spherical	H_2O_2 Detection	Yang *et al.* 2015
Eucalyptus globulus	$AgNO_3$	Leaf	1.9–4.3	Spherical	Antibacterial, Antibiofilm	Ali et al. 2015
Cranberry	$AgNO_3$	Fruit	2.8 ± 2.1, 1.4 ± 0.8, 8.6 ± 2.5	Spherical	Antimicrobial	Ashour *et al.* 2015
Phyllanthus niruri	$AgNO_3$	Leaf	30–60	Spherical	Mosquitocidal	Suresh *et al.* 2015
Zingiber officinale	$AgNO_3$	Broth extract	3.1	Spherical	Antibacterial	Shalaby et al. 2015
Tagetes erecta	$AgNO_3$	Flower	10–90	Irregular, exagonal and Spherical	Antimicrobial	Padalia *et al.* 2015
Oak	$AgNO_3$	Fruit	40	Cubic and Spherical	Cytotoxic	Heydari and Rashidipour, 2015
Trilobata	$AgNO_3$	Leaf	-	-	-	Billacura and Mimbesa *et al.* 2015
Azadirachta indica	$AgNO_3$	Leaf	34	Spherical	Antibacterial and Photolumine scence	Ahmed *et al.* 2016
Coffea arabica	$AgNO_3$	Seed	20-30	Spherical	Antibacterial	Dhand *et al.* 2016
Terminalia arjuna	$AgNO_3$	Bark	2-100	Spherical	Antimicrobial	Ahmed *et al.* 2016
Catharanthus roseus	$AgNO_3$	Leaf	20	Spherical	-	Al-Shmgani *et al.* 2016
Prunus japonica	$AgNO_3$	Leaf	26	Hexagona, Trigonal, Spherical	-	Saravanakumar *et al.* 2016
Excoecaria agallocha	$AgNO_3$	Leaf	-	Hexagonal, Spherical	Antibacterial,	Bhuvaneswari *et al.* 2016

					Antioxidant and Cytotoxic	
Artocarpus altilis	$AgNO_3$	Leaf	38	Spherical	Antimicrobial, Antioxidant	Ravichandran *et al*. 2016
Terminalia cuneata	$AgNO_3$	Leaf	25–50	Irregular	Catalytic	Edison *et al.* 2016
Ficus benghalensis	$AgNO_3$	Bark	60	Spherical	Antibacterial, Antiproliferative	Nayak *et al*. 2016
Phoenix Dactylifera	$AgNO_3$	Leaf	20–60	Irregular	Catalytic	Aitenneite *et al.* 2016
Capuli cherry	$AgNO_3$	Fruit	20-80	Spherical	Antioxidant	Kumar *et al.* 2016
Mussaenda glabrata	$AgNO_3$	Leaf	51.32	Spherical	Antimicrobial, Antioxidant, Catalytic	Francis *et al*. 2016
Cowpea seeds	$AgNO_3$	Seed	70	Spherical	-	Mohammadi *et al*. 2016
Apple	$AgNO_3$	Fruit	30.25 ± 5.26 nm	Spherical	Antibacterial	Ali *et al.* 2016
Artemisia absinthium	$AgNO_3$	Leaf	5 to 20 nm	Polydispersed	-	Ali *et al.* 2016
Artemisia absinthium	$AgNO_3$	Leaf	5-20	Spherical	-	Ramachandran *et al*. 2016
Citrus lemon	$AgNO_3$	Fruit	2-10	Spherical	-	Mosae *et al*. 2016
Peumus boldus	$AgNO_3$	Leaf	18	Spherical	-	Sánchez *et al*. 2016
Echinochloa colona	$AgNO_3$	Leaf	50-70	Spherical	-	Lakshman *et al.* 2016
Salvinia molesta	$AgNO_3$	Seed	12.46	Spherical	Antibacterial	Verma *et al.* 2016
Sesbania grandiflora	$AgNO_3$	Leaf	16	Spherical	Antimicrobial	Ajitha *et al*. 2016
Polyalthia longifolia	$AgNO_3$	Leaf	13.9	Anisotropic	Antioxidant	Kumar *et al.* 2016
Pedalium murex	$AgNO_3$	Leaf	50	Spherical	Antibacterial	Anandalakshmi *et al*. 2016
Allamanda cathartica	$AgNO_3$	Flower	-	Spherical	Antioxidant, Antibacterial	Karunakaran *et al*. 2016
Manihot esculenta	$AgNO_3$	Leaf	-	Spherical	Larvicidal	Velayutham *et al.* 2016
Bougainvillea spectabilis	$AgNO_3$	Flower	16-83	Spherical	Antibacterial	Bharathi *et al.* 2016
Clausena anisata	$AgNO_3$	Leaf	60.67	Spherical	Antioxidant	Begum *et al*. 2016
Aegiceras corniculatum	$AgNO_3$	Leaf	23-72	Irregular	Cytotoxic	Kumar *et al.* 2016
Tecomella undulata	$AgNO_3$	Leaf	3-18	Spherical	-	Chaudhuri *et al*. 2016
Osmanthus	$AgNO_3$	Flower	2-30	Spherical	-	Dong *et al.* 2016

fragrans						
Pimpinella anisum	$AgNO_3$	Seed	80-85	Spherical	Cytotoxic	Devanesan *et al.* 2017
Camella sinesis	$AgNO_3$	Leaf	7	Spherical	Sensing	Silva-De Hoyos *et al.* 2017
Alysicarpus monilifer	$AgNO_3$	Leaf	15 ± 2	Spherical	Antibacterial	Kasithevar *et al.* 2017
Tamarind	$AgNO_3$	Fruit	10	Spherical	Antibacterial	Jayaprakash *et al.* 2017
Elephantopus scaber	$AgNO_3$	Leaf	37.86	Irregular	Antibacterial	Francis *et al.* 2017
Turmeric	$AgNO_3$	Rhizome	120-160	-	Antibacterial	Nayak *et al.* 2017
Carissa carandas	$AgNO_3$	Fruit	23 ± 2	-	Catalytic	Anupama *et al.* 2017
Lycium barbarum	$AgNO_3$	Fruit	3-15	Spherical	-	Dong *et al.* 2017
Gmelina arborea	$AgNO_3$	Fruit	8-32	Spherical	Catalytic	Saha, *et al.* 2017
Viburnum opulus	$AgNO_3$	Fruit	25	Spherical	Anti-inflammatory	Moldovan *et al.* 2017
Citrullus lanatus	$AgNO_3$	Fruit	17.96 ± 0.16	Spherical	-	Ndikau *et al.* 2017
Momordica charantia	$AgNO_3$	Fruit	10-50	Spherical	Antmicrobial	Supraja *et al.* 2017
Rubus crataegifolius	$AgNO_3$	Fruit	13	Anisotropic	Catalytic	Rokade *et al.* 2017
Excoecaria agallocha	$AgNO_3$	Fruit	-	Spherical	Antibacterial	Nagababu *et al.* 2017
Rheum palmatum	$AgNO_3$	Root	121 ± 2	Hexagonal, Spherical	-	Arokiyaraj *et al.* 2017
Diospyros sylvatic	$AgNO_3$	Root	8	Irregular	Antibacterial	Pethakamsetty, *et al.* 2017
Bauhinia variegata	$AgNO_3$	Leaf	-	-	Larvicidal	Govindarajan *et al.* 2017
Pongamia pinnata	$AgNO_3$	Seed	16.4	Spherical	-	Beg *et al.* 2017
Mangifera indica	$AgNO_3$	Leaf	-	-	Antibacterial	Sarsar, *et al.* 2017
Arbutus unedo	$AgNO_3$	Leaf	58, 40	Spherical	Antibacterial	Skandalis *et al.* 2017
Tribulus longipetalus	$AgNO_3$	Leaf	15	Irregular	Antioxidant and Antibacterial	Djahaniani *et al.* 2017
Datura stramonium	$AgNO_3$	Leaf	15–20	Spherical	Antimicrobial	Gomathi, *et al.* 2017
Melissa officinalis	$AgNO_3$	Leaf	12	Spherical	Antimicrobial	de Jesús Ruíz-Baltazar *et al.* 2017
Chenopodium aristatum	$AgNO_3$	Stem	3-36	quasi-spherical	Catalytic, Antibacterial	Yuan *et al.* 2017
Pongamia pinnata	$AgNO_3$	Seed	16.4	-	Antibacterial, Medicinal	Beg *et al.* 2017
Artemisia	$AgNO_3$	Leaf	25	Spherical	Biomedical	Rasheed, *et al.* 2017

vulgaris						
Crocus sativus L	$AgNO_3$	Petals	15	Spherical	Antibacterial	Bagherzade, *et al*. 2017
Cassia auriculata	$AgNO_3$	Flower	10-35	Spherical, Triangular	Catalytic	Muthu, *et al*. 2017
Eriobotrya japonica	$AgNO_3$	Leaf	20	Spherical	Antibacterial	Rao *et al*. 2017
Syzygium jambos	$AgNO_3$	Leaf and Bark	8.51 ± 1.63, 5.58 ± 1.84	Spherical and Ellipsoidal	Antibacterial, Cytotoxic	Dutta *et al.* 2017
Physalis angulata	$AgNO_3$	Leaf	11-96	Irregular	Antibacterial, Antioxidant	Kumar *et al.* 2017
Morus nigra	$AgNO_3$	Leaf	4-8	Spherical	Antifungal	Hafez *et al.* 2017
Waste Tea	$AgNO_3$	-	45	Spherical	Catalytic, Antibacterial	Qing *et al.* 2017
Syzygium aromaticum	$AgNO_3$	-	5-20	Spherical	Cytotoxic	Venugopal *et al*. 2017
Achillea millefolium L	$AgNO_3$	kernel shell	20	-	Catalytic	Khodadadi *et al*. 2017
Excoecaria agallocha L	$AgNO_3$	Leaf	23-42	Spherical, Hexagonal	Antibacterial, Antioxidant, Cytotoxic	Bhuvaneswari *et al*. 2017
Tecomella undulata	$AgNO_3$	Leaf	3-18	Spherical	-	Chaudhuri *et al*. 2016

Likewise, the fruit of *Carissa carandas* and *Lycium barbarum* were utilized by Anupama and Madhumitha and Dong *et al*. for the synthesis of AgNPs. The study revealed that the obtained AgNPs were 23 ± 2 and 3-15 nm in size respectively. The AgNPs synthesized from *Carissa carandas* exhibited excellent catalytic activity (Anupama and Madhumitha 2017, Dong *et al*. 2017). The fruits of *Gmelina arborea*, *Viburnum opulus*, *Citrullus lanatus*, and *Momordica charantia* also showed the excellent synthesis potential for spherical AgNPs. The results indicated that the size of the obtained AgNPs were 8-32, 25, 17.96 ± 0.16, and 10-50 nm respectively (Saha *et al*. 2017, Moldovan *et al*. 2017, Ndikau *et al*. 2017, Supraja *et al*. 2017). Rokade *et al*. have reported the synthesis of anisotropic AgNPs with average size 13 nm using the fruit extract of *Rubus crataegifolius* which showed the catalytic activity (Rokade *et al*. 2017). Nagababu and Rao also used fruit extract of

Excoecaria agallocha and reported the synthesis of spherical shaped AgNPs for antibacterial activity (Nagababu and Rao 2017). The root of *Rheum palmatum* was investigated against the synthesis potential of AgNPs. The results obtained after the characterization indicated that the AgNPs were hexagonal and spherical shaped with average size 121±2 nm (Arokiyaraj *et al*. 2017). The root of *Diospyros sylvatic* was also used by Pethakamsetty *et al*. which showed the synthesis of irregular shaped AgNPs with average size 8 nm (Pethakamsetty *et al*. 2017). AgNPs synthesized from the leaf extract of *Bauhinia variegate* corroborated larvicidal activity (Govindarajan *et al*. 2016). Beg *et al*. have used the seed of *Pongamia pinnata* and synthesized the spherical AgNPs having average size 16.4 nm (Beg *et al*. 2017). Similarly, several other plants have also been used in recent years by several authors for the synthesis of AgNPs which are given in **Table 1.8.**

The first report on the formation of AuNPs by plant was reported by Gardea-Torresdey *et al*. 2002 inside the living alfalfa plant. Thus obtained AuNPs were anisotropic in the range of 2-20 nm. By synthesizing the AuNPs, they have opened the new and exciting way to obtain the AuNPs. They have also provided an excellent link between material science and biotechnology in the growing field of bionanotechnology (Gardea-Torresdey *et al*. 2002). Thereafter, the synthesis of AuNPs was reported by Shankar *et al*. and Armendariz *et al*. using leaf extracts of *Azadirachta indica* and *Avena sativa* in the size range of 5-30 nm and 5-85 nm respectively (Shankar *et al*. 2004, Armendariz *et al*. 2004). Shankar *et al*. have also reported the preparation of anisotropic AuNPs using lemon grass (Shankar *et al*. 2005). The green synthesis of AuNPs was carried out using *Tamarind* and *Emblica officinalis* by using leaves and fruits respectively (Ankamwar *et al*. 2005a, Ankamwar *et al*. 2005b). Chandran *et al*., Ghule *et al*., and Singh *et al*. have shown the green synthesis of AuNPs

using *Aloe vera*, *Cicer arietinum*, and *Cymbopogon flexuosus* (Chandran *et al*. 2006, Ghule *et al*. 2006, Singh *et al*. 2006). Sharma *et al*. 2007 and Huang *et al*. 2007 have used root and leaves extracts of the *Sesbania drummondii* and *Cinnamomum camphora* and synthesized AuNPs in the size range of 6-20 nm and 15-25 nm respectively (Sharma *et al*. 2007, Huang *et al*. 2007). The leaf extracts of *Camelia sinensis* and *Coriandrum sativum* showed their great potential towards the formation of AuNPs with the size of 40 nm and 6.7–57.9 nm respectively (Vilchis-Nestor *et al*. 2008, Narayanan and Sakthivel 2008). Ramezani *et al*. 2008 have used the leaf extracts of *Eucalyptus camaldulensis*, and *Pelargonium roseum* and synthesized spherical AuNPs in the range of 1.2-17.5 nm and 2.5-27.5 nm respectively (Ramezani *et al*. 2008). Similarly, Begum *et al*., Raghunandan *et al*., Wang *et al*., Kasthuri *et al*., and Smitha *et al*., have utilized the leaf extract of *Black tea*, *Psidium guajava*, *Scutellaria barbata*, *Henna*, and *Cinnamomum zeylanicum* respectively (Begum *et al*. 2009, Raghunandan *et al*. 2009, Wang *et al*. 2008, Kasthuri *et al*. 2009, Smitha *et al*. 2009). Philip investigated the reducing capability of *Hibiscus rosa sinensis* for the synthesis of AuNPs. The results showed the synthesis of different shaped AuNPs like triangular, hexagonal, dodecahedral and spherical with the average size of 14 nm (Philip 2010b). Dwivedi and Gopal have reported the synthesis of AuNPs uing the leaf extracts of *Chenopodium album* and (Dwivedi and Gopal 2010). Ankamwar 2010 have showed the green synthesis of AuNPs using *Terminalia catappa* (Ankamwar 2010).

Das *et al*. have reported the green synthesis of different shaped AuNPs using *Centella asiatica* in the size range of 2-22 nm (Das *et al*. 2010). Dubey *et al*. 2010 have carried out the green synthesis of AuNPs using the leaf extracts of *Rosa rugosa*, *Sorbus aucuparia*, and fruit extracts of *Tanacetum vulgare* (Dubey *et al*. 2010a, Dubey *et al*. 2010b, Dubey *et al*. 2010c).

Table 1.9 List of different plants and their parts used in the synthesis of AuNPs

Plants	Precursor	Parts of the plant	Size (nm)	Morphology	Application	Reference
Medicago sativa	$HAuCl_4$	Seed	2-20	Anisotropic	-	Gardea-Torresdey *et al*. 2002
Pelargonium graveolens	$HAuCl_4$	Leaf	20-40	Decahedral, Icosahedral		Shankar *et al*. 2003
Azadirachta indica	$HAuCl_4$	Leaf	5-30	Spherical,Triangular, Hexagonal	-	Shankar *et al*. 2004
Avena sativa	$HAuCl_4$	Stem	5-85	Triangular, Spherical	-	Armendariz *et al*. 2004
Lemongrass	$HAuCl_4$	Leaf	200-500	Spherical, Triangular, Hexagonal	-	Shankar *et al*. 2005
Tamarind	$HAuCl_4$	Leaf	20-40	Triangular, Hexagonal and Spherical	Vapor Sensing	Ankamwar *et al*. 2005
Emblica officinalis	$HAuCl_4$	Fruits	15-25	Spherical, Triangular, Twinned decahedral	-	Ankamwar *et al*. 2005
Aloe vera	$HAuCl_4$	Leaf	50-350	Spherical, Triangular, Hexagonal	-	Chandran *et al*. 2006
Cicer arietinum	$HAuCl_4$	Seeds	25	Spherical, triangular	-	Ghule *et al*. 2006
Cymbopogon flexuosus	$HAuCl_4$	Leaf	15-200	Hexagonal, Triangular, Spherical	Vapor Sensing	Singh *et al*. 2006
Sesbania drummondii	$HAuCl_4$	Root	6-20	Spherical	Catalytic	Sharma *et al*. 2007
Cinnamomum camphora	$HAuCl_4$	Leaf	15-25	Spherical, Plate like		Huang *et al*. 2007
Camelia sinensis	$HAuCl_4$	Leaf	40	Spherical, Triangular	-	Vilchis-Nestor *et al*. 2008
Eucalyptus camaldulensis , *Pelargonium rose um*	$HAuCl_4$	Leaf	1.2-17.5, 2.5-27.5	Spherical	-	Ramezani *et al*. 2008
Coriandrum sativum	$HAuCl_4$	Leaf	6.7–57.9	Spherical, Triangular, Decahedral	-	Narayanan *et al*. 2008
Black tea	$HAuCl_4$	Leaf	20	Nano-prisms, Nano-rods and Nano-trapezoids	-	Begum *et al*. 2009
Psidium guajava	$HAuCl_4$	Leaf	25-30	Spherical	-	Raghunandan *et al*. 2009
Scutellaria barbata	$HAuCl_4$	-	5-30	Spherical and Triangular	Electrochemistry	Wang *et al*. 2009
Magnolia kobus and *Diopyros kaki*	$HAuCl_4$	Leaf	5-300	Triangular, Pentagonals Hexagonal and Spherical	-	Song *et al*. 2009
Henna	$HAuCl_4$	Leaf	9-70	Spherical, Triangular	-	Kasthuri *et al*. 2009
Phyllanthus amarus	$HAuCl_4$	Leaf	10-110	Spherical, Hexagonal,	-	Kasthuri *et al*. 2009

				Triangular, Rod		
Cinnamomum zeylanicum	$HAuCl_4$	Leaf	25	Spherical, Triangular	-	Smitha *et al*. 2009
Hibiscus rosa sinensis	$HAuCl_4$	Leaf	14	Triangular, Hexagonal, Dodecahedral and Spherical	-	Philip *et al*. 2010
Chenopodium album	$HAuCl_4$	Leaf	10-30	Spherical, Triangular	-	Dwivedi *et al*. 2010
Syzygium aromaticum	$HAuCl_4$	buds	5-100	Crystalline, Irregular, Spherical, Elliptical	-	Raghunandan *et al*. 2010
Terminalia catappa	$HAuCl_4$	Leaf	10-35	Spherical	-	Ankamwar *et al*. 2010
Centella asiatica	$HAuCl_4$	Leaf	2-22	Triangular, Hexagonal Spherical	-	Das *et al*. 2010
Rosa rugosa	$HAuCl_4$	Leaf	50-250	Spherical	-	Dubey *et al*. 2010
Sorbus aucuparia	$HAuCl_4$	Leaf	50-150	Hexagonal, Triangular Spherical	-	Dubey *et al*. 2010
Tanacetum vulgare	$HAuCl_4$	Fruit	11	Spherical, Triangular	-	Dubey *et al*. 2010
Magnifera Indica	$HAuCl_4$	Leaf	20-70	Spherical	-	Phillip *et al*. 2010
Pear	$HAuCl_4$	Fruit	200-500	Triangular, Hexagonal	-	Ghodake *et al*. 2010
Dioscorea bulbifera	$HAuCl_4$	Tubers	11-30	Spherical	-	Ghosh *et al*. 2011
Zingiber officinale	$HAuCl_4$	Rhizome	5-15	Spherical	Blood compatibility	Kumar *et al*. 2011
Anacardium occidentale	$HAuCl_4$	Leaf	6.5, 17	Spherical	-	Sheny *et al*. 2011
Murraya koenigii	$HAuCl_4$	Leaf	20	Spherical, Triangular	-	Philip *et al*. 2011
Ocimum sanctum	$HAuCl_4$	Leaf	30	Hexagonal, Triangular and Spherical	-	Philip *et al*. 2011
Mentha piperita	$HAuCl_4$	Leaf	150	Spherical	Antibacterial	MubarakAli *et al*. 2011
Nyctanthes arbortristis	$HAuCl_4$	Flower	19.8±5	Spherical	-	Das *et al*. 2011
Maduca longifolia	$HAuCl_4$	Leaf	7	Hexagonal, Triangular, Spherical	Infrared absorption	Fayaz *et al*. 2011
Cacumen Platycladi	$HAuCl_4$	Leaf	7.4±0.8	Spherical	-	Zhan *et al*. 2011
Memecylon edule	$HAuCl_4$	Leaf	20-50	Spherical, Cylindrical, rod	-	Elavazhagan *et al*. 2011
Swietenia mahogini JACQ	$HAuCl_4$	Leaf	100 nm	Spherical, Triangular	-	Mondal *et al*. 2011
Mucuna pruriens	$HAuCl_4$	-	6-17.7	Spherical	-	Arulkumar *et al*. 2011

Rosa hybrida	$HAuCl_4$	Petal	10	Triangular, Hexagonal and Spherical	-	Noruzi *et al.* 2011
Macrotyloma uniflorum	$HAuCl_4$	Leaf	14-17	Spherical	-	Aromal *et al.* 2012
Sapindus mukorossi	$HAuCl_4$	Shells	9-19	Spherical	Catalytic	Reddy *et al.* 2012
Terminalia chebula	$HAuCl_4$	Seed	6-60	Spherical	-	Kumar *et al.* 2012
Cypress	$HAuCl_4$	Leaf	5-80	Spherical	-	Noruzi *et al*.2012
Trigonella foenum-graecum	$HAuCl_4$	Seed	15-20	Spherical	Catalytic	Aromal *et al.* 2012
Abelmoschus esculentus	$HAuCl_4$	Seed	45-75	Spherical	Antifungal	Jayaseelan *et al*. 2013
Terminalia arjuna	$HAuCl_4$	Leaf	20	Spherical	cell division and pollen germination	Gopinath *et al*. 2013
Memecylon umbellatum	$HAuCl_4$	Leaf	15-25	Hexagonal, Triangular, Spherical	Anti microbial	Arunachalam *et al*. 2013
Citrus limon, Citrus reticulata and *Citrus sinensis*	$HAuCl_4$	Fruits	15±20, 17±50, 18±60	Spherical, Triangular	-	Sujitha *et al*. 2013
Hovenia dulcis	$HAuCl_4$	Fruit	15-20	Hexagonal, Spherical	-	Basavegowda *et al*. 2014
Acalypha indica	$HAuCl_4$	Leaf	20-30	Spherical	-	Krishnaraj *et al*. 2014
Blackberry, blueberry, pomegranate	$HAuCl_4$	Fruit	20-500	Spherical, Triangular	-	Nadagouda *et al*. 2014
Angelica, Hypericum and *Hamamelis*	$HAuCl_4$	Roots, bloomy herba and bark	3-4	Spherical, Oval Polyhedral	-	Pasca *et al*. 2014
Garcinia Combogia	$HAuCl_4$	Fruit	12	Spherical, Triangular, Rod	Catalytic	Rajan *et al*. 2014
Phoenix dactylifera L. (Palmae)	$HAuCl_4$	Leaf	32-45	Spherical	Catalytic	Zayed *et al*. 2014
Lippia citriodora, Salvia officinalis, Pelargonium graveolens, Punica granatum	$HAuCl_4$	Leaf	1-8, 30-70	Spherical, Triangular		Elia *et al*. 2014

Curcuma pseudomontana	$HAuCl_4$	Rhizomes	20	Spherical	cytotoxicity	Muniyappan *et al*. 2014
Acacia nilotica	$HAuCl_4$	Bark	30	Quasi-spherical, Anisotropic	Detection of nitrobezene	Emmanuel *et al*. 2014
Plumbago zeylanica	$HAuCl_4$	Root	20-30	Spherical, Triangular	Biofilm control	Salunke *et al.* 2014
Mulberry	$HAuCl_4$	Leaf	15-53	Spherical	Antibacterial	Adavallan *et al*. 2014
Molenga oleifera	$HAuCl_4$	Flower	3-5	Spherical, Hexagonal, Triangular	Anticancer and catalytic	Anand *et al*. 2015
Cymbopogon citratus	$HAuCl_4$	Leaf	20-50	Spherical, Hexagonal Triangular, Rod	Mosquitocidal	Murugan *et al*.2015
Pogestemon benghalensis	$HAuCl_4$	Leaf	10-50	Triangular, Spherical	Photocatalytic degradation of dye	Paul *et al*. 2015
Vetiveria zizanioides and *Cannabis sativa*	$HAuCl_4$	Root and leaf	10-35	Spherical	Antifungal	Swain *et al*. 2016
Hibiscus sabdariffa	$HAuCl_4$	leaf	10-60	Spherical	Cytotoxicity	Mishra *et al*. 2016
Panax ginseng	$HAuCl_4$	Root	10-40	Spherical	Antibacterial	Singh *et al.* 2016
Peltophorum pterocarpum	$HAuCl_4$	Flower	5-50	Spherical	-	Balamurugan. *et al.* 2016
Carica papaya, Catharanthus roseus and mixed	$HAuCl_4$	Leaf	3.5-9, 2-20, 6-18	Spherical, Triangular	Antitumar, antibacterial	Muthukumar *et al*. 2016
Mimusops elengi	$HAuCl_4$	Bark	9-14	Spherical	Catalytic	Majumdar *et al*. 2016
Dendropanax morbifera	$HAuCl_4$	Leaf	10-20	Polygon, Hexagon, Spherical	Anticancer	Wang *et al*. 2016
Camellia sinensis, J. communis and *Green coconut*	$HAuCl_4$	Leaf	40-70, 20-30, 30-70	Spherical, Triangular Hexagonal, Rod	-	Geraldes *et al*. 2016
Cordia myxa	$HAuCl_4$	Fruit	20-50	Spherical, Pentagonal, Triangular, Hexagonal	-	Ankamwar *et al*. 2017
Eucalyptus oleosa	$HAuCl_4$	Leaf	28	Spherical	Antioxidant	Pourmortazavi *et al.* 2017
Elettaria cardamomum	$HAuCl_4$	Seed	15.2	Spherical	Antioxidant, antibacterial	Rajan *et al*. 2017
Sphaeranthus indicus	$HAuCl_4$	Leaf	25	Spherical	Cell division, Pollen	Balalakshmi *et al*. 2017

					germination	
Mussaenda glabrata	$HAuCl_4$	Leaf	44.1±0.82	Spherical, Triangular	Catalytic	Francis *et al.* 2017
Citrus maxima	$HAuCl_4$	Fruit	25.7±10	Spherical, Rod	Catalytic	Yu *et al*. 2017

Leaf extracts of *Magnifera Indica* and fruit extacts of *Pear* were also investigated for their synthesis potential of AuNPs (Philip 2010a, Ghodake *et al*. 2010). The tuber of *Dioscorea bulbifera* and rhizome of *Zingiber officinale* also were successfully showed the great synthesizing potential for the spherical AuNPs in the size range of 11-30 and 5-15 nm respectively (Ghosh *et al*. 2011, Kumar *et al*. 2011). The leaf extracts of *Anacardium occidentale*, *Murraya koenigii*, *Ocimum sanctum*, *Mentha piperita* were also used for the green synthesis of AuNPs (Philip *et al*. 2011, Sheny *et al*. 2011, Philip and Unni 2011, MubarakAli *et al*. 2011). Similarly several authors have reported the green synthesis of AuNPs using different parts of the plants which are given in **Table 1.9** (Mondal *et al*. 2011, Das *et al*. 2011, Fayaz *et al*. 2011b, Zhan *et al*. 2011, Elavazhagan and Arunachalam 2011, Arulkumar and Sabesan 2011, Noruzi *et al*. 2011, Aromal *et al*. 2012, Reddy *et al*. 2012, Kumar *et al*. 2012b, Noruzi *et al*. 2012, Aromal and Philip 2012, Jayaseelan *et al*. 2013, Gopinath *et al*. 2013, Arunachalam *et al*. 2013, Sujitha and Kannan 2013, Basavegowda *et al*. 2014, Krishnaraj *et al*. 2014, Nadagouda *et al*. 2014, Pasca *et al*. 2014, Rajan *et al*. 2014, Zayed and Eisa 2014, Elia *et al*. 2014, Muniyappan and Nagarajan 2014, Emmanuel *et al*. 2014, Salunke *et al*. 2014, Adavallan and Krishnakumar 2014, Anand *et al*. 2015, Murugan *et al*. 2015, Paul *et al*. 2015b, Swain *et al*. 2016, Mishra *et al*. 2016, Singh *et al*. 2016, Balamurugan *et al*. 2016, Muthukumar *et al*. 2016, Majumdar *et al*. 2016, Wang *et al*. 2016, Geraldes *et al*. 2016)

Recently, Ankamwar *et al*. Pourmortazavi *et al*. have used the fruit and leaf extract of *Cordia myxa* and *Eucalyptus oleosa* respectively for the potent synthesis of AuNPs (Pourmortazavi *et al*. 2017, Ankamwar *et al*. 2017). Rajan *et al*. 2017 and Balalakshmi *et al*. 2017 have reported the green synthesis of spherical AuNPs using seed extract of *Elettaria cardamomum* and leaf extract of *sphaerathus indicus*. They observed that the synthesized AuNPs were spherical in shape with average size 15.2 and 25 nm respectively (Rajan *et al*. 2017, Balalakshmi *et al*. 2017). The leaf extract of *Mussaenda glabrata* have showed the synthesis of spherical and triangular AuNPs which corroborated greater catalytic activity towards the degradation of dye (Francis *et al*. 2017). The fruit extracts of *Citrus maxima* was used for the synthesis of spherical and rod shaped AuNPs with the average size of 25.7±10 nm.

1.4.2.1 Photoinduced synthesis

Although, the green synthesis of AgNPs and AuNPs using plant extracts was more economical and eco-friendly than other biological routes, but still the consumption of long time duration and energy while heating and stirring was its huge limitation. Therefore, it was needed to be modified with energy and time efficient route. The photoinduced synthesis of AgNPs and AuNPs using plant extracts avoided the use of energy and time consumption. Hence it has become a completely economical and eco-friendly route for the size controlled biosynthesis of the AgNPs and AuNPs where the rate of biosynthesis is increased by natural sunlight. There are several articles which have been published for the biosynthesis of AgNPs using sunlight induced route. Zarchi *et al*. have reported the rapid biosynthesis of AgNPs using ethanol extract of *Andrachnea chordifolia* via sunlight-induced route (Zarchi *et al*. 2011). Dong *et al*. produced a stepwise synthesis of AuNPs under solar radiation (Dong *et al*.

2004). Biosynthesis of AgNPs was reported by Sahu *et al*. using an aqueous extract of *Cynodon dactylon* under bright sunlight radiation (Sahu *et al*. 2013).

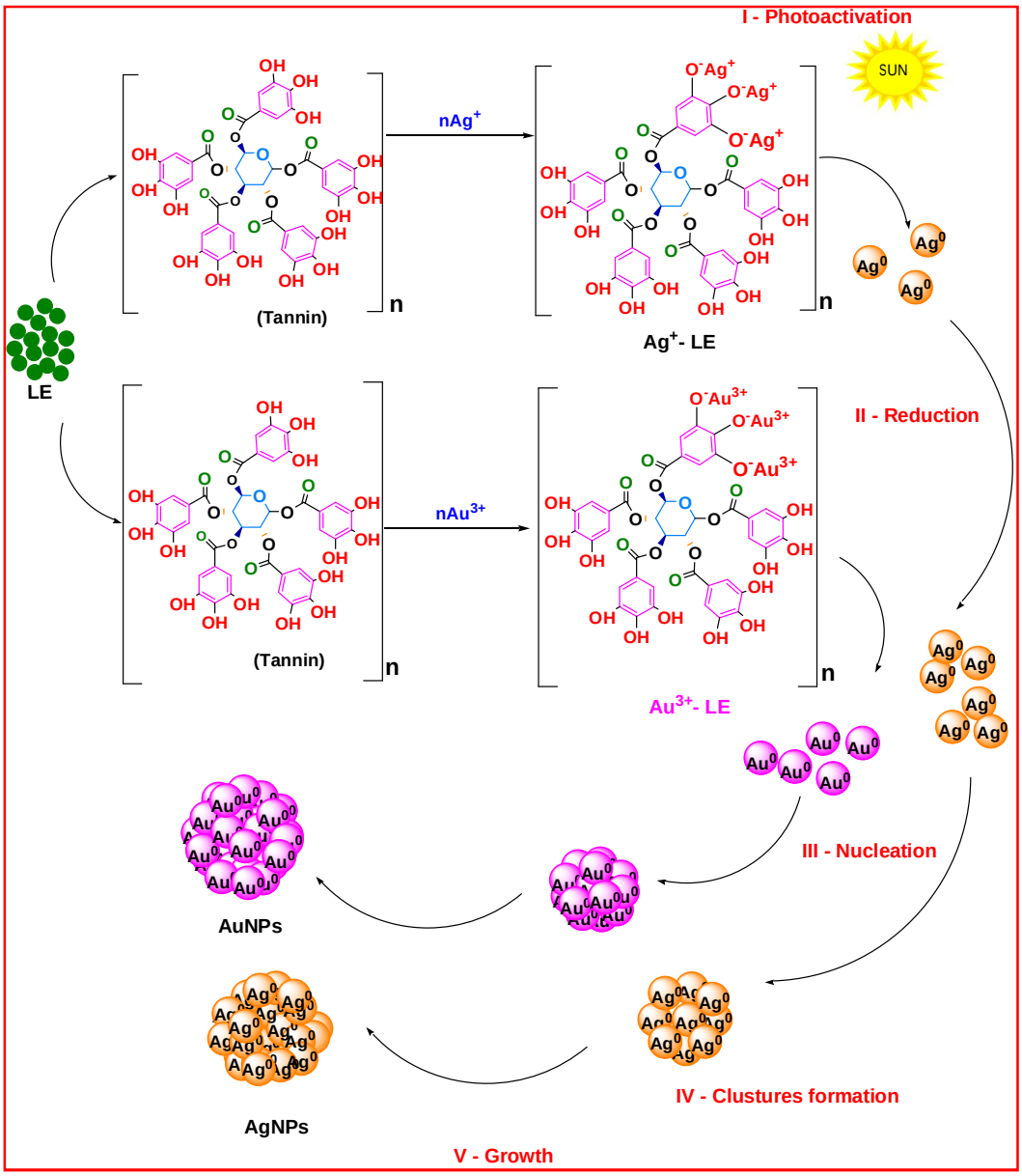

Scheme 1.5 Illustration of the different steps of photoinduced synthesis of AgNPs and AuNPs

We have also reported the photoinduced synthesis of AgNPs using aqueous extract of *Croton bonpnandianum* (Kumar *et al*. 2017b), *Erigeron bonariensis* (Kumar *et al*. 2016c), *Xanthium*

strumarium (Kumar *et al*. 2016d), *Murraya koenigi* (Kumar *et al*. 2017c), and *Physalis angulata* (Kumar *et al*. 2017d).

The photoinduced synthesis of AgNPs and AuNPs using leaf extract (LE) is mediated by the involvement of hydrated electrons released form the metal ions (Ag^{+} Au^{3+}) and LE complex upon irradiation. When the LE is added into the metal ion solution, the OH group of polyphenolic compound (for example, tannin) present in LE bound with metal ions (Ag^{+} Au^{3+}) and formed the Ag^{+}/Au^{3+}-LE complex. The first step involves the photoactivation of Ag^{+}/Au^{3+} - LE complex. The second step involves the release of hydrated electrons by debonding of OH group of LE after absorbing the photons of light (Yang *et al*. 2015, Zhou *et al*. 2014, Pal and Pal 1999). The third step involves the reduction of Ag^{+} and Au^{3+} to Ag^{0} and Au^{0} respectively by the hydrated electrons produced earlier (Sakamoto *et al*. 2009). In the fourth step, the Ag^{0} and Au^{0} nucleates to form nanoclusters which are followed by the fifth step where the formation of AgNPs and AuNPs occurrs by the aggregation of nanoclusters (**Scheme 1.5**).

1.5 Properties of AgNPs and AuNPs

AgNPs and AuNPs exhibit extraordinary properties than metallic silver and gold respectively which made them excellent to be used in various applications. These properties are:

1.5.1 Tunable shape and size

The AgNPs and AuNPs possess several important physicochemical properties such as tunable size (surface area), shape, surface charge, etc. which are very important for determining their biological interactions and impacts.

Table 1.10 Relationship between the diameter, surface area, volume and surface area to volume ratio (https://nanocomposix.com/pages/silver-nanoparticles-physical-properties**)**

Nanoparticles Diameter (nm)	Surface area (nm^2)	Volume (nm^3)	Surface Area:Volume
10	314	523	0.60
20	1260	4190	0.30
30	2830	14100	0.20
40	5030	33500	0.15
50	7850	65500	0.12
60	11300	113000	0.10
70	15400	180000	0.09
80	20100	268000	0.08
90	25400	382000	0.07
100	31400	523600	0.06

It is well documented that smaller nanoparticles have a larger surface area and, therefore, have greater toxic potential. AgNPs and AuNPs have unique properties due to their small size.

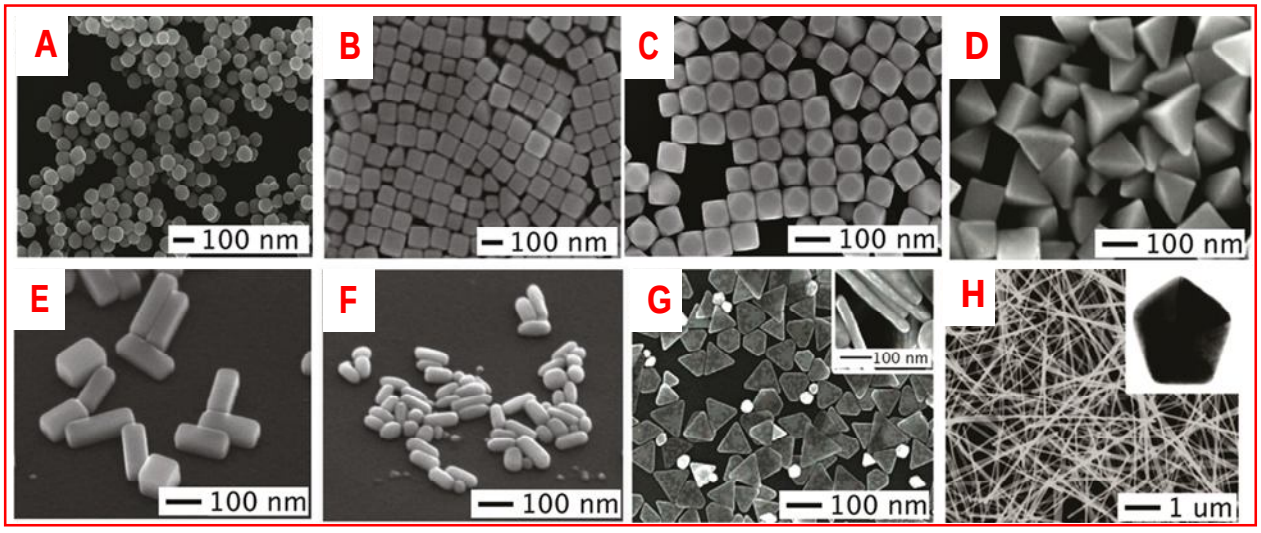

Figure 1.4 Different nanostructures of AgNPs (A) spheres, (B) cubes, (C) truncated cubes, (D) right bipyramids, (E) bars, (F) spheroids, (G) triangular plates, and (H) wires (Rycenga *et al*. 2011)

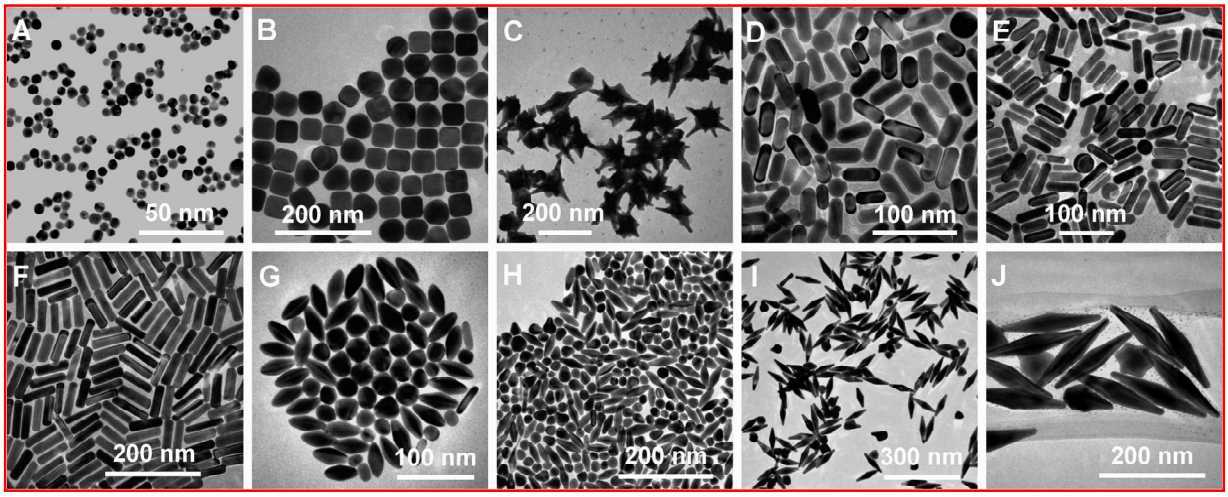

Figure 1.5 Different nanostructures of AuNPs (A) spheres, (B) cubes, (C) nanobranches, (D) nanorods (aspect ratio) = 2.4 ± (0.3), (E) nanorods (aspect ratio) = 3.4 ± (0.5), (F) nanorods (aspect ratio) = 4.6 ± (0.8), (G) nanobipyramids (aspect ratio) = 1.5 ± (0.3) (H) nanobipyramids (aspect ratio) = 2.7 ± (0.2), (I) nanobipyramids (aspect ratio) = 3.9 ± (0.2), (J) nanobipyramids (aspect ratio) = 4.7 ± (0.2) (Chen *et al.* 2008)

All nanoparticles regardless of their chemical constituents have extremely high surface area: volume ratios (**Table 1.10**). Thus, many of the physical properties of the nanoparticles such as solubility and stability are dominated by the nature of the nanoparticle surface. For comparison, a regular size baseball has a diameter of 73,000,000 nm, a surface area of 16,800,000,000,000,000 nm^2, and a volume of 204,000,000,000,000,000,000,000 nm^3. The surface area to volume ratio is 0.00000008, a factor of 7,500,000 less than 10 nm nanoparticles.

Rycenga *et al*. have prepared different nanostructures of AgNPs like spheres, cubes, truncated, bipyramids, bars, spheroids, triangular plates, and wires which are shown in **Figure 1.4** (Rycenga *et al*. 2011). Similarly, Chen *et al*. have also prepared different nanostructures of AuNPs (Chen *et al*. 2008) (**Fig.1.5**).

1.5.2 Charged surface

Studies have found that the biological effects of AgNPs depend on the different surface charges of their coatings, which can affect the interaction of AgNPs with living systems (Powers *et al*. 2011). Chang *et al*. have shown that cationic trimethyl chitosan nitrate-capped AgNPs (TMCN-AgNPs) have a positive surface charge and display high storage stability at the room temperature. They also found that the TMCN-AgNPs with positively charged surfaces killed Gram-positive, Gram-negative, and *Acinetobacter baumannii* strains at very low concentrations (Chang *et al*. 2017).

1.5.3 Excellent stability

The stability of the nanoparticles can be explained through three conceptions: electrostatic, steric and their combined electrostatic repulsive forces.

1.5.3.1 Electrostatic stabilization

The concept of electrostatic stabilization originated from the repulsive electrostatic force which is experienced by nanoparticles surrounded by a double layer of electric charges. The DLVO theory states that the nanoparticles are stable when the electrostatic repulsion dominates the attractive van der Waals forces (Freitas and Müller 1998). The sum of attractive forces (van der Waals) and repulsive forces (due to a double layer of counter ions) gives an idea of total energy potential (V_T) which determines the stability of the nanoparticles. It is considered that when the kinetic energy (E_k) of particle motion is less than V_T, the particles are stable whereas the particles are unstable when the E_k is greater than V_T (Kraynov and Müller 2011). It is assumed that the approach of negatively charged anions (rather than positive cations) to a metal sphere induces a partial positive charge (δ +) on the surface (**Figure 1.6 A**).

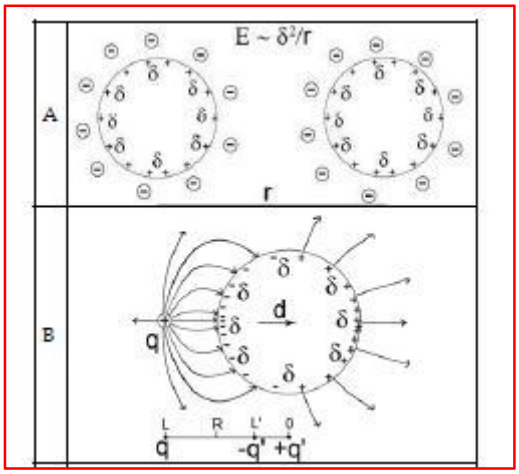

Figure 1.6 Schematic representation of (A) coulomb repulsion between partially charged particles as the origin of electrostatic stabilization, (B) neutral metal sphere having radius 'R' showing the distribution of the surface charge and geometry of the electric field, when the adsorbate is a single external charge 'q' in the distance 'L' from the centre. The electric potential of this system is equivalent to the superposition of the potential of an external point charge q and the induced dipole moment 'd' (Kraynov and Müller 2011)

Equally "charged" particles repel each other, which is the basis of general electrostatic stabilization (Ott and Finke 2007, Özkar and Finke 2002). However, the above description does not adqeuately consider the redistribution of electron charge density on the metal sphere. Let us assume that an external charge q approaches the surface of a neutral non-grounded metal sphere (**Figure 1.6 B**). Note that this implies that the overall electric charge of this sphere is zero and remains so. Close to the approaching charge, an excess of surface charges (with opposite sign) accumulates, whereas excess charges of opposite sign appear on the other side of the sphere (Landau and Lifshitz 1982).

1.5.3.2 Steric stabilization

The concept of the steric stabilization is based on the steric repulsion between molecules or ions which get adsorbed on neighboring particles. The extent of stabilization is

based on size and chemical nature of these molecules. The large and bulky molecules provide an efficient stabilization due to the geometric constraints around nanoparticles.

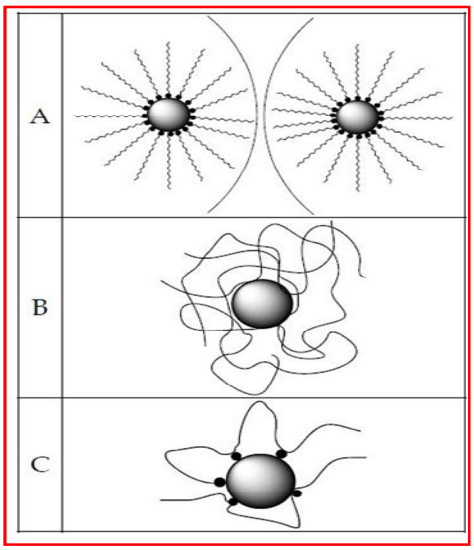

Figure 1.7 Schematic illustrations of steric stabilization (A) elongated or conical molecules adsorbed *via* anchoring centres (small black dot) hinder nanoparticles from close contact, (B) long polymer threads encapsulate a nanoparticle, (C) chelate effect, when the stabilizer is adsorbed *via* more than one anchoring centre (small black dots)

For the approaching nanoparticles, the elongated or conical geometry is advantageous to keep them apart (**Figure 1.7 A**). The nanoparticles get encapsulated into a sphere when the length of the stabilizing agent is significantly longer than its size. A sphere can be formed encapsulating the nanoparticle as represented in (**Figure 1.7 B**). Therefore, high molecular weight polymers are often employed as stabilizers for nanoparticles.

To provide long residence time and to prevent the spontaneous desorption of the nanoparticle, the stabilizers are needed to be adsorbed strongly enough on its surface. When the stabilizer gets adsorb on the surface of nanoparticles from several centers, the chelating effect enhances the adsorption of the stabilizers on its surface (**Figure 1.7 C**). The frequent driving force for strong binding between the stabilizers and metal surface is chemisorption.

Metals with more valence orbitals than valence electrons have an "electron deficient" surface. Thus, molecules readily "donating" electron density (i.e., with chemical groups associated with free electron lone pair, such as divalent sulphur, trivalent phosphorus, and trivalent nitrogen moieties or molecules with π-electrons, e.g., aromatic systems) often adsorb very strongly on metal surfaces (although the opposite examples are also known) (Temirov *et al*. 2006). Strongly adsorbing, large molecules are prime candidates for stabilization of nanoparticles.

Nanoparticles are either charge-stabilized or sterically stabilized. The stability of the charge-stabilized nanoparticles is measured by zeta potential. The nanoparticles having zeta potentials greater than 20 mV or less than -20 mV have sufficient electrostatic repulsion which provides them sufficient stability in solution. The nanoparticles can dissolve into ionic form in highly acidic or basic condition. Highly acidic or basic solutions can also increase the dissolution rate of the nanoparticles into an ionic form that can plate onto the sides of the container or re-deposit onto existing nanoparticles changing the average diameter and size distribution. AgNPs are also susceptible to light (especially ultraviolet light) and should be stored in the dark.

1.5.4 Easy functionalization

AgNPs and AuNPs can be functionalized very easily using various ligands. Some of them act as both reducing and stabilizing agent. The surface functionalization strategies of the nanoparticles are the prerequisite for the targeted applications since they affect its stability. Ravindran *et al*. have stabilized AgNPs using bovine serum albumin (BSA) via chemisorption for the biosensing application (Ravindran *et al*. 2010). Thiol has an extremely strong affinity towards both AgNPs and AuNPs. Naik *et al*. used peptides for synthesis and stabilization of AgNPs (Naik

et al. 2002). Mondal *et al*. used cysteine and lysine to prepare water dispersible AgNPs and AuNPs (Mandal *et al*. 2001). Michael Faraday was the first who prepared gold hydrosol by the reduction of an aqueous solution of chloroaurate using phosphorus (Faraday 1857). Turkevich was the first who used citrate as both reducing and stabilizing agent for the synthesis of AuNPs (Turkevich *et al*. 1951). Thereafter, alkanethiol was employed by Mulvany *et al*. which was followed by Brust and Schiffrin in 1994 who reported two-phase synthesis strategy using thiol-gold interaction to stabilize AuNPs. After that several ligands, polymers were used to functionalize the AuNPs. The commonly used polymers are polyvinylpyrrolidone (PVP), polyethylene glycol (PEG), polyvinyl alcohol (PVA), polyvinyl methyl ether (PVME), chitosan, polyethyleneimine (PEI), polydiallyl dimethyl ammonium chloride (PDDA), and polymethylmethacrylate (PMMA) etc. Some other sulfur-containing ligands used for the protecting AuNPs are disulfides, di and trithiols, thioethers, xanthates, and resorcinarene tetrathiols. Iodine can be used to oxidize and decompose these thiol-stabilized AuNPs. 167 Amine-capped AuNPs were reported using primary amines (Saha *et al*. 2012).

1.5.5 Biocompatibility

The AgNPs and AuNPs are most biocompatible nanoparticles because they are composed of inert material. Connor *et al*. have shown that AuNPs incorporated into human cell did not cause any toxicity (Connor *et al*. 2005). Similarly, Pauksch *et al*. studied the biocompatibility of AgNPs on the mesenchymal stem cells and osteoblasts by adding 10 μg/g of AgNP and incubated for 21 days. He did not observe any effect on the differentiation of these cells (Pauksch *et al*. 2014).

1.5.6 Surface plasmon resonance (SPR)

Surface plasmon resonance is the significant optical property of AgNPs and AuNPs which results from the collective oscillation of free conduction electron after interaction with electromagnetic waves of visible light (Wei *et al*. 2015). This collective oscillation of the free conduction electrons is very sensitive to changes in the size and shape of the nanoparticle. The energy required to collectively excite the motion of the surface plasmon electrons increases with the decrease in diameter of the nanoparticles (Knoll 1998). For example, the energy required to excite the surface plasmon electron is comparable to the energy of visible light for AuNPs having diameters of 5 nm. Therefore, AuNPs strongly absorb with a maximum absorbance at wavelengths near 520 nm. AuNPs with diameters larger than 5 nm strongly absorbs with a maximum absorbance towards longer wavelengths. Thus one can tune the maxima of the SPR absorbance between 520 nm to 1000 nm (i.e., right from the visible into the near-infrared) by changing the diameter of the nanoparticle. Therefore, SPR of AgNPs and AuNPs result in strong visible and near-infrared (NIR) scattering and absorption. In addition to this, the SPR band is also sensitive to change in the dielectric properties of the surrounding medium (Kurihara and Suzuki 2002). Media of high dielectric constants (refractive indices) are effectively more polarizable and thus coupled with the surface plasmon electrons more readily, and the energy required to excite the electrons collectively is decreased. That is, the maximum in the SPR absorbance shifts to lower energy (longer wavelengths). In this context, the nanoparticles have an inherent sensing ability.

1.6 Applications of AgNPs and AuNPs

Due to extraordinary properties like tunable shape and size, biocompatibility, high surface plasmon resonance, AgNPs and AuNPs are being widely used in several applications such as antimicrobial, cytotoxicity, sensing, catalysis, drug delivery, wound healing, etc.

1.6.1 Antibacterial

AgNPs and AuNPs are widely used nanomaterials for their potent antibacterial activity. When the bacterial cultures are exposed to the AgNP and AuNPs, primarily the Ag^+ ions and Au^+ are released into aqueous solution following partial oxidation (Chaloupka *et al*. 2010). These ions after interacting with the plasma membrane, interfere with the cellular functions like permeability and respiration, and ultimately killed the cells by lysis. AgNPs and AuNPs also prevent the replication of DNA and synthesis of protein by binding with DNA or by denaturing ribosomes (Chaloupka *et al*. 2010). Cui *et al*. have explained the detailed study of antibacterial activity against *E. coli*. The antibacterial activity of the nanomaterials depends on the structure of cell wall. On the basis of cell wall structure, the bacteria are classified into two major groups; Gram-negative (having a thick layer of peptidoglycans) and Gram-positive (having a thin layer of peptidoglycan). The Gram-positive bacteria are affected strongly comparatively Gram-negative bacteria. Dhand *et al*. have shown the effective antibacterial activity of AgNPs synthesized from *Coffea arabica* seed (Dhand *et al*. 2016). Abdel-Raouf *et al*. have investigated the antibacterial activity of both AuNPs synthesized from *Galaxaura elongata* (Abdel-Raouf *et al*. 2017).

1.6.2 Antifungal

Bahrami-Teimoori *et al*. have reported the green synthesis of AgNPs (10-32 nm) using the extract prepared from the leaves of *Amaranthus retroflexus* and they investigated

its antifungal activity against the plant pathogenic fungi such as *Macrophomina phaseolina, Alternaria alternata* and *Fusarium oxysporum* (Bahrami-Teimoori *et al*. 2017). Narayan and Park have demonstrated the antifungal activity of AgNPs synthesized from turnip leaf extract against the wood-degrading fungal pathogens such as *Gloeophyllum abietinum, G. trabeum, Chaetomium globosum*, and *Phanerochaete sordid* (Narayanan and Park 2014).

AgNPs and AuNPs are also used as antifungal agents. Swain *et al*. have used root and leaf extracts of *Vetiveria zizanioides* and *Cannabis sativa* for the synthesis of AuNPs which showed an excellent potential towards antifungal activity (Swain *et al*. 2016). *Abelmoschus esculentus* seed extract was utilized by Jayaseelan *et al*. for the green synthesis of AuNPs with size ranging from 45-75 nm. Thus obtained AuNPs were investigated for the antifungal activity against *Puccinia graminis, Aspergillus flavus, Aspergillus niger* and *Candida albicans* using standard well diffusion method (Jayaseelan *et al*. 2013). Wani *et al*. have investigated size dependent antifungal activity of AuNPs which exhibited excellent antifungal activity against the fungus, *Candida*. They observed that discs shaped AuNPs corroborated stronger antifungal activity as compared to polyhedral shaped AuNPs (Wani and Ahmad 2013).

1.6.3 Antiviral

Although, the viruses are very serious for agriculture and human health, but still there are very few reports available on the antiviral activity of AgNPs and AuNPs. For example, the antiviral activity of the AgNPs synthesized by *Aspergillus ochraceus* was investigated by Vijaykumar and Prasad where they used the plaque count method to determine the effectiveness against M13 phage (Vijayakumar and Prasad 2009). Gaikwad *et al*. reported the mycomediated synthesis of AgNPs which showed the antiviral activity against herpes

simplex virus and human parainfluenza virus type 3 (Gaikwad *et al*. 2013). Sujitha *et al*. have used *Moringa oleifera* seed extract for the synthesis of AgNPs which showed great antiviral activity against dengue serotype DEN-2 and its major vector *Aedes aegypti* (Sujitha *et al*. 2015). The antiviral activity of AuNPs was also reported by some authors. Kesarkar *et al*. have synthesized AuNPs and observed its entry inhibitory as well as neutralizing activity against HIV virus (Kesarkar *et al*. 2017). Baram *et al*. have used mercaptoethanesulfonate functionalized AuNPs (MES-AuNPs) as effective inhibitors of Herpes simplex virus type 1 infection which was based on its ability to mimic cell-surface-receptor heparan sulfate (Baram-Pinto *et al*. 2010).

1.6.4 Anticancer

Several authors have reported the cytotoxicology studies of AgNPs and AuNPs against various cancer cell lines. Venugopal *et al*. have synthesized AgNPs in the range of 5-20 nm from *Syzygium aromaticum* and investigated its cytotoxicity activity against breast cancer cell line (MCF-7) and breast cancer cell line (A549) (Venugopal *et al*. 2017). The AgNPs synthesized from the leaf extract of *Ficus religiosa* with average size 21 nm was investigated for the cytotoxic study on different cell lines (Nakkala *et al*. 2017). Jacob *et al*. have used the dried fruits of *Ficus carica* for the green synthesis of AgNPs which showed anticancerous activity on MCF-7 (Jacob *et al*. 2017). Jang *et al*. have used aqueous flower extract of *Lonicera hypoglauca* as reducing and capping agents for the synthesis of AgNPs and applied it in In vitro anticancer activity on MCF-7 (Jang *et al*. 2016). The cytotoxic study of AgNPs and AuNPs synthesized from *Spinacia oleracea* was investigated by Ramachandran *et al*. on mouse myoblast cancer cell line (Ramachandran *et al*. 2017).

Similarly, Naraginti and Li reported the anticancerous activity of AgNPs and AuNPs synthesized from *Actinidia deliciosa* (Naraginti and Li 2017).

1.6.5 Catalytic

Green synthesized AgNPs and AuNPs have also been used as a catalyst in several decontamination based reactions. The beet root extract mediated synthesis of AgNPs also showed good catalytic activity against the degradation of 4-Nitro phenol (Bindhu and Umadevi 2015). Tahir *et al*. reported the catalytic degradation of methylene blue using AgNPs synthesized from extract of *Salvadora persica* (Tahir *et al*. 2015). Aromal and Philip reported the green synthesis of AuNPs using the extract of *Trigonella foenum-graecum* and investigated its size-dependent catalytic activity. They observed that smaller AuNPs showed better catalytic activity than larger AuNPs (Aromal and Philip 2012). *Breynia rhamnoides* derived AgNPs and AuNPs showed potent catalytic activity for the degradation of 4-Nitro phenol to 4-Amino phenol (Gangula *et al*. 2011).

1.6.6 Biosensing

Green synthesized AgNPs and AuNPs are also being used as a biosensor for the colorimetric detection of several water pollutants. For example; Annadhasan *et al*. have utilized green synthesized AgNPs and AuNPs. They observed that the synthesized AgNPs were sensitive for the colorimetric detection of Hg^{2+} and Mn^{2+} whereas AuNPs were sensitive for Hg^{2+} and Pb^{2+} (Annadhasan *et al*. 2014). Annadhasan and Rajendiran reported highly sensitive and selective colorimetric detection of Hg^{2+} using AgNPs synthesized from green route (Annadhasan and Rajendiran 2015). The sensitive and selective detection of Hg^{2+} was also reported by Kumar *et al*. using aqueous extract of *Muraaya koienigii* (Kumar *et al*. 2017c). Basiri *et al*. have synthesized AgNPs using *Cucumis melo* juice. Thus obtained

AgNPs were further utilized for the colorimetric detection of Cu^{2+} (Basiri *et al*. 2017). Kumar *et al*. also showed the colorimetric detection of Iron (III) using AgNPs synthesized from *Croton bonlandianum* (Kumar *et al*. 2017b). The green synthesized AgNPs were also capable of detecting the cysteine from serum samples as reported by Shen *et al*. (Shen *et al*. 2016) Balavigneswaran *et al*. have prepared AgNPs using aqueous leaf extract of Anacardium occidentale for the rapid detection of chromium (IV) (Balavigneswaran *et al*. 2014). Joshi *et al*. have synthesized AgNPs through *S. aromaticum* and investigated the pH controlled detection of chromium (IV) (Joshi *et al*. 2016).

1.6.7 Drug delivery

The investigation of the biological effect of the nanoparticles is very important for the effective drug delivery system. Since AgNPs and AuNPs have unique physical and chemical properties as well as strong binding affinity towards thiols, amino acids, proteins, carboxylic acid aptamers and disulfides, therefore these are being used extensively in the field of drug delivery (Khan *et al*. 2014). Kumar and Poornachandra have studied the in vitro release of Miconazole from Miconazole-AgNPs which was evaluated in phosphate buffer saline (PBS) at pH 5.5 and 7.4 for 6 h. they observed that 90% of the Miconazole was released at pH 5.5 whereas only 30% release was observed at pH 7.4 (Kumar and Poornachandra 2015). The curcumin-loaded AgNPs hydrogel prepared by Ravindra *et al*. was studied against antibacterial activity and drug delivery application. It was found that the modified AgNPs showed a controlled release of curcumin and significantly active against *E. coli* as compared to normal AgNPs (Ravindra *et al*. 2012). Paciotti *et al*. have studied the drug delivery using PEG-modified AuNPs where they target tumor cells by extravasation using AuNPs coated with a mixture of tumor necrosis vector and PEG-thiol (Paciotti *et al*. 2004). Light-controlled

external release strategy was used by Yeh *et al*. to deliver the anticancer drug 5-fluorouracil into cells using AuNPs functionalized with monolayer of zwitterionic and photocleavable ligands on the surface (Yeh *et al*. 2012).

1.6.8 Gene delivery

Since last decade, AuNPs has emerged out as an excellent candidate for the delivery of small drug molecules or large biomolecules such as DNA and siRNA. Generally, gene therapy is meant for the treatment and control of diseases by the use of nucleic acids. Guo *et al*. have reported that charge reversal polyelectrolyte deposited AuNPs effectively enhanced the gene delivery efficiency and gene expression in the context of RNA interference (Guo *et al*. 2010). Niidome *et al*. have prepared AuNPs using $NaBH_4$ in the presence of 2-aminoethanethiol which formed a complex structure with plasmid DNA containing a luciferase gene. This complex particle could be used to deliver a gene into the target HeLa cells in about 3 h (Niidome *et al*. 2004). Umeda *et al*. have reported that the combination of phototherapy with conventional gene has improved the efficiency of gene delivery into cells (Umeda *et al*. 2005). The work reported by Niidome *et al*. revealed the release of plasmid DNA from AuNPs after exposing to pulsed laser irradiation (Niidome *et al*. 2004).

1.6.9 Wound healing

AgNPs and AuNPs have been used extensively in wound healing applications, due to their strong antibacterial activity. So far, several studies have been done on the wound healing property of AgNPs and AuNPs. Wright *et al*. have investigated the wound healing property of AgNPs coated dressing material on wound created on the backs of pigs which were contaminated with *Pseudomonas aeruginosa*, *Fusobacterium* sp., staphylococci, by covering with dressing material containing AgNPs and without AgNPs. They observed the

rapid wound healing in first few days of post-injury in the wound covered by dressing material containing AgNPs (Wright *et al*. 2002). The study on AgNPs impregnated bacterial cellulose (AgNPs-BC) was carried out by Wu *et al*. where they found that the slow release of AgNPs from AgNPs-BC exhibited excellent antibacterial activity with 99% reductions in *E. coli*, *S. aureus*, and *P. aeruginosa* which can be used as wound healing material (Wu *et al*. 2014). Recently, Lu *et al*. have reported the preparation of spongy AgNPs nanocomposite which showed enhanced wound healing property (Lu *et al*. 2017). The wound healing property of AuNPs in photobiomodulation therapy (PBMT) was investigated by Lau *et al*. which showed its much potential to accelerate wound healing due to enhanced epithelialization, collagen deposition and fast vascularization (Lau *et al*. 2017). Sivakumar *et al*. investigated the wound healing efficacy of AgNPs and AuNPs synthesized from *Brassica oleracea* L using a mouse model. They observed that both AgNPs and AuNPs showed a great potential towards wound healing without showing any toxic effects (Sivakumar *et al*. 2017).

1.7 Selection of plant source

Generally, the weed plants grow in stress condition which led them to synthesize secondary metabolites like polyphenolics such as tannin, flavonoids, terpenoids, alkaloids, enzymes, protein, sugars, etc. These secondary metabolites are the rich source of reducing and stabilizing agent which can reduce silver and gold metal ion into AgNPs and AuNPs.

In the current study, several plants present in our Institute campus (Indian Institute of Technology, Banaras Hindu University, Varanasi, 221005, Uttar Pradesh, India) were investigated against the synthesis of AgNPs and AuNPs but due to the rich source of secondary metabolites, the weed plants; *Xanthium strumarium* (*X. strumarium*) and *Croton*

bonplandianum (*C. bonplandianum*) were used as a source of reducing and stabilizing agents.

1.7.1 *Xanthium strumarium*

X. strumarium is an annual plant species and belongs to Asteraceae family. It is commonly known as cocklebur. This is a gregarious weed found throughout the India having the maximum length up to 1 m in height with a short, stout, hairy stem and commonly found in stress condition, along roads, canals and river banks (Kamboj *et al*. 2010). *X. strumarium* is a self-fertile plant and its flowering time in India is August-September. The flowers are monoecious and are pollinated by insects. The major route of seed dispersal is through animal which gets stick with the skin and hairs of the animals as the fruits have hooked bristles and two strong hooked beaks.

X. strumarium is considered as a reputed medicine in several parts of the world including Europe, China, Indo-China, Malaysia, and America. The root and fruits of this plant are used as a medicine. The Ayurveda advocates that *X. strumarium* has numerous medicinal properties like cooling, fattening, alexiteric, anthelmintic, tonic, laxative, digestive and antipyretic. It also improves appetite, voice, complexion, and memory. It is also used in curing of leucoderma, biliousness, a bite of poisonous insects, epilepsy, salivation, and fever. It is reported to be fatal to cattle and pigs (Kamboj *et al*. 2010). The American tribes use it to relieve constipation, diarrhea and vomiting. The phytochemical study of this plant revealed the presence of various phytochemicals such as alkaloids, flavonoids, triterpenoids, terpenoids, tannin, saponin, quinone, protein, and sugars (Farooq *et al*. 2014). *X. strumarium* L. fruits are used in traditional Chinese medicine for the treatment of sinusitis, rheumatism and skin pruritus; from this source a novel thiazinedione derivative has been

reported (Ma *et al*. 1998). The extracts from its various parts showed antifungal, anti-inflammatory, antileishmanial, antitrypanosomal, hypoglycemic, anthelmintic, antiulcerogenic, diuretic, and anticancer activities (Kandhare *et al*. 2012; Sharifi *et al*. 2015). In our study, the leaf extract of *X. strumarium* was investigated for its potential of rapid biosynthesis of AgNPs and AuNPs.

1.7.1.1 Scientific classification of *X. Strumarium*

Kingdome: Plantae

Division: Magnoliophyta

Class: Magnolopsida

Order: Asterales

Family: Asteraceae

Genus: Xanthium

Species: *X. strumarium*

Botanical Name - *Xanthium strumarium*

Figure 1.8 *X. strumarium* plant showing the leaves and fruits

1.7.2 *Croton bonplandianum*

C. bonplandianum, is a perennial herb belonging to family Euphorbiaceae. It is a native weed to the Southern Bolivia, Paraguay, Southwestern Brazil and Northern Argentina (Vennila *et al*. 2010). It is also found in India as an exotic weed and commonly found along the roads, canal, and other water stressed area. *C. bonplandianum* is commonly known as Kala Bhangra (Hindi), three-leaved caper (English), Ban Tulsi, Jungle Tulsi (Bengali), Eliamanakku (Tamil), Kukka mirapa (Telgu), Alpa bedhi soppu (Kannada). Flowering and fruiting time of *C. bonplandianum* is September to December (Thenmojhi *et al*. 2013). *C. bonplandianum* has a great medicinal value in Indian Ayurveda. The seeds of this plant are used to cure jaundice, abdominal dropsy, acute constipation, and internal abscesses (Reddy 1995). The extracts obtained from the various parts of this plant have potent antimicrobial and antitumor activity. This plant is also considered as chologogue and purgative. The fresh juice prepared from the leaves of this plant is used for the treatment of headache (Saggoo *et al* 2010). The latex of plants shows the healing of the wounds and cut. The plant has been credited with potential to cure the liver disorder, swelling of the body, cure against ringworms and skin diseases.

In spite of having medicinal value it has a great composition of reducing as well as capping agent required for the potent biosynthesis of AgNPs (Singh *et al*. 2014). *C. bonplandianum*, commonly known as Three-Leaved Caper.

1.7.2.1 Scientific classification of *C. bonplandianum*

Kingdome: Plantae

Division: Magnoliophyta

Class: Magnolopsida

Order: Euphorbiales

Family: Euphorbiaceae

Genus: Croton

Species: *C. bonplandianum*

Botanical Name- *C. bonplandianum*

Figure 1.9 *C. bonplandianum* plant showing the leaves, flowers, and fruits

1.8 Research objectives

The above mentioned background information from the exhaustive literature survey enlightened the fact of deep exploration of green synthesis using plant extracts. It encouraged for the development of completely eco-friendly and economically viable green route for the rapid synthesis of AgNPs and AuNPs without utilizing the external source of energy like heating and stirring. Therefore, it is necessary to develop such a route to explore the optimum synthesis of AgNPs and AuNPs by optimizing the various process parameters affecting the synthesis such as time, leaf extract dose, and metal ion concentration. Thus in the current study, following objectives were set to explore the optimum synthesis of AgNPs and AuNPs, characterization and further utilization in environmental and biological applications.

- ❖ Selection of suitable plant containing phytochemicals such as tannin, alkaloids, flavonoids, sugar, proteins, enzymes, etc.
- ❖ Development of one pot, eco-friendly, economically viable and energy efficient route for the swift synthesis of AgNPs and AuNPs.
- ❖ Optimization of different process variable affecting the synthesis of AgNPs and AuNPs such as exposure time, leaf extract dose, metal ion concentration.

a. UV-visible spectroscopy
b. Fourier Transform Infrared Spectroscopy (FT-IR) analysis
c. X-Ray Diffraction (XRD) analysis
d. Scanning Electron Microscopy (SEM) Analysis
e. Energy-dispersive X-Ray spectroscopy (EDS) analysis
f. Transmission Electron Microscopy (TEM) Analysis
g. Selected Area Diffraction Pattern (SAED) Analysis
h. Atomic Force Microscopy (AFM) Analysis
i. X-Ray Photoelectron Spectroscopy (XPS) analysis

- Utilization of thus obtained AgNPs and AuNPs at an optimum condition for the environmental and biological applications